DISSERTATION

Identification of ABI1, new carbon/nitrogen regulator regulates plant C/N response via new pathways in *Arabidopsis*, and functional characterization of conventional C/N regulators, ATL31 and 14-3-3 in tomato (*Solanum lycopersicum* L.)

（シロイヌナズナにおける新規炭素/窒素栄養バランス制御因子 ABI1 の単離と既知の炭素/窒素制御因子 ATL31 と 14-3-3 のトマト果実形成における機能解析）

Submitted by

Yu LU

Biosystems Science Course

Graduate School of Life Science

In partial fulfillment of the requirements

For the Degree of Doctor of Philosophy in Life Science

Hokkaido University

Sapporo, Japan

March 2017

TABLES OF CONTENTS

SUMMARY IN JAPANESE

Identification of ABI1, new carbon/nitrogen regulator regulates plant C/N response via new pathways in *Arabidopsis*, and functional characterization of conventional C/N regulators, ATL31 and 14-3-3 in tomato (*Solanum lycopersicum L*.)

（シロイヌナズナにおける新規炭素/窒素栄養バランス制御因子 ABI1 の単離と既知の炭素/窒素制御因子 ATL31 と 14-3-3 のトマト果実形成における機能解析）

地表に固定され生きる植物は，生息環境に適応するために，多様な環境情報を感知し，応答する優れた能力を有する。私は，植物の栄養環境，特に利用可能な糖（炭素源，C）と窒素（N）量のバランス「C/N」に注目し，研究を進めてきた。シロイヌナズナでは，高炭素/低窒素（高 C/低 N）培地で，子葉の緑化が抑制される一方，アントシアニンを蓄積し，発芽後成長が著しい阻害を受ける。このような現象では，炭素および窒素の絶対量ではなく，その相対的バランスが重要であり，「C/N 応答」と称される。C/N は，発芽後成長に限らず，花成や老化の進行にも影響し，植物のライフサイクル転換点において重要なシグナルとなる。C/N 応答は，古くからその重要性が認識されている一方で，その制御メカニズムは不明のままであった。本研究では植物の C/N 応答制御機構の解明を目指して、モデル植物シロイヌナズナおよびモデル作物種であるトマトを用いた，下記二つの解析に取組んだ。

1. 新規 C/N 応答制御因子 CNI2/ABI1 の単離と機能解析

C/N 応答機構の分子実態を明らかにすることを目的に，シロイヌナズナ FOX（Full-length cDNA OvereXpression）ラインを用いた C/N 応答異常変異体のスクリーニングを行った。その結果，新規 C/N 応答異常変異体 *cni2-D (carbon/nitrogen insensitive 2-D)* を単離した。*cni2-D* 変異体は，野生型が著しい生育阻害を受けるような高 C/低 N 培地でも子葉が緑化し生育できた。さらに原因遺伝子について解析した結果，この変異体は，*ABI1* 遺伝子の過剰発現により，C/N ストレス耐性になっていた。一方，ABI1 機能欠損変異体は C/N ストレスに真逆の過剰応答を示すことから，CNI2/ABI1 が C/N 応答制御因子として重要であることが確認できた。ABI1 は植物ホルモンのアブシジン酸（ABA）シグナル伝達系の負の制御因子として機能する脱リン酸化酵素である。ABI1 は，脱リン酸化標的である SnRK2 キナーゼ群の活性を制御することにより，下流に広がる広範なリン酸化カスケードおよび遺伝子発現を制御する。さらに，ABI1 自身の活性は，ABA 受容体（PYR/RCAR）との直接結合により負の制御を受けており，ABA シグナル伝達系の最上流に位置する重要な制御因子である。このことから，ABA シグナル伝達系は C/N 応答機構にも関与することが示唆された。ただし，興味深いことに，通常条件と高 C/低 N ストレス条件において植物体内の ABA 含量の差は検出されなかった。また，既知

の糖および ABA シグナル伝達因子である *ABI4* や *ABI5* の変異体は C/N 応答に異常を示さなかった。一方，ABI1 の新たな脱リン酸化標的として報告されはじめた SnRK1 キナーゼ（Rodrigues et al., 2013, Plant Cell）のリン酸化状態は C/N で変動した。実際，SnRK1 経路の下流マーカー遺伝子の発現は，野生型では C/N ストレス時に低下し，一方で *ABI1* 過剰発現体では非感受性となることが分かった。これらの結果から，ABI1 は，既存の ABA および糖シグナル伝達系とは異なり，SnRK1 を介した新規のシグナル伝達経路を介して C/N 栄養応答を制御することが示唆された。

2. トマト果実における CNI1/ATL31 および 14-3-3 タンパク質の機能解析

上記 CNI2/ABI1 の単離に先立ち，当研究室の先行研究から，C/N 応答制御因子 CNI1 として新規ユビキチンリガーゼ ATL31 が単離された。加えて，そのユビキチン化標的として 14-3-3 タンパク質が同定された。これまでの解析から，ATL31 はユビキチンリガーゼとして機能し，ユビキチン化標的である 14-3-3 タンパク質の安定性制御を介して，植物の C/N 応答を制御することが明らかになっている。ATL ファミリーは，多様な植物種に広く保存された膜局在型ユビキチンリガーゼであるが，シロイヌナズナ以外の植物種における機能はほとんど分かっていない。また，14-3-3 は，特異的なリン酸化モチーフを認識・結合することで，代謝酵素やトランスポーター，転写因子等の多様なタンパク質の機能制御を果たすことが知られている。14-3-3 もまた，植物種を超えて高度に保存されているが，果実の形成・成熟における機能は未知である。本研究課題では，これまでシロイヌナズナを用いて研究してきた C/N 応答制御因子 ATL31 および 14-3-3 機能解析を，モデル作物種のトマト果実を用いた解析に発展させた。

その結果，トマトにおける *ATL31* ホモログ遺伝子(*SlATL31*)を単離し，SlATL31 タンパク質がユビキチンリガーゼ活性を有することが確認された。また，SlATL31 はトマト 14-3-3 タンパク質と結合することが示されたことから，シロイヌナズナ ATL31 と同様の生化学的機能を有することが示唆された。さらに，トマト果実における 14-3-3 複合体のアフィニティー精製と MS 解析による 14-3-3 標的因子の網羅的同定に成功した。この MS 解析結果から，14-3-3 がトマト果実の成熟過程において，糖代謝や細胞壁合成に関する重要な酵素群を標的因子として制御することが示唆された。トマト果実の成熟過程におけるタンパク質翻訳後修飾による酵素活性制御に関する情報はほとんど得られておらず，この研究成果は，トマト果実の収量および栄養成分を最適化するための基盤情報となることが期待される。

上記の研究課題から，植物の C/N 栄養応答に関する新規制御因子を単離し，C/N 栄養シグナルに関する新たな制御経路の存在を突き止めた。さらに，これまでのモデル植物シロイヌナズナの発芽後成長解析から得られた C/N 応答制御因子について，作物種トマトの果実形成における機能解析へと発展させることで，植物 C/N 応答解析の農学的応用への道を拓いた。

ACKNOWLEDGEMENTS

First of all, I would like to express my deepest gratitude to Prof. Junji Yamaguchi and Dr. Takeo Sato for constant encouragement and guidance throughout not only my research but as well as my life in Japan.

Secondly, high tribute shall be paid to Drs. Yoichiro Fukao (Ritsumeikan University, Japan), Takashi Hirayama (Okayama University, Japan) and Izumi C. Mori (Okayama University, Japan) for experimental collaboration; Dr. Hironori Kaminaka (Tottori University, Japan) for technical advice regarding yeast two-hybrid assay and providing the related materials; Drs. Shoji Mano (National Institute for Basic Biology, Japan) and Yoshihisa Ueno (National Institute of Agrobiological Science, Japan) for providing the Gateway destination vectors; Drs. Chiaki Matsukura (Tsukuba University, Japan) and Hiroshi Ezura (Tsukuba University, Japan) for providing transgenic tomato; Drs. Takayuki Tohge (Max-Planck-Institute of Molecular Plant Physiology, Germany) and Alisdair R. Fernie (Max-Planck-Institute of Molecular Plant Physiology, Germany) for providing valuable discussion and excellent collaboration.

Thirdly, special thanks should go to Drs. Yukako Chiba, Shugo Maekawa, Huihui Sun, Yosuke Maruyama, Yuya Suzuki, Lorenzo Guglielminetti and Thais Huarancca Reyes for technical advice and in-depth discussion.

Finally, I am also greatly thankful to all members of my laboratory for their assistance, help, and friendliness. I am also indebted to my mother and my wife for endless encouraging and selfless supporting.

This work was supported by the Ministry of Education, Culture, Sports, Science, and Technology (MEXT) as part of Joint Research Program implemented at the Institute of Plant Science and Resources, Okayama University in Japan, and Cooperative Research Grant of the Plant Transgenic Design Initiative, Gene Research Center, the University of Tsukuba and the production of transgenic tomato plants was supported by the RIKEN Plant Transformation Network. ‘Micro-Tom’ seeds were provided by the Gene Research Center, University of Tsukuba, through the National Bio-Resource Project, MEXT, Japan. Proteomic analysis was sup- ported by Center for Food and

Medical Innovation. I was supported by a Special Grant Program for Young Foreign Scientists in Basic Science (Hokkaido University Faculty of Science: 2014– 2015), MEXT Honors Scholarship for Privately Financed International Students (2015) and research fellowships from the Japan Society for the Promotion of Science (2016–2018).

PREFACE

In order to adapt to the constantly fluctuated environment, plants have evolved a sophisticated mechanism for precisely sensing and ingeniously responding to these challenges. Nutrient availability in the environment profoundly restricts plant growth, especially carbon and nitrogen, by providing energy sources and structural components, are essential elements for all living organisms. Besides of their structural fundamental significance, they also participate in the regulation of many aspects of plant physiology via a role of signaling molecular that triggers specific respective signaling pathways[1,2,3]. It has been proposed that, in addition to the absolute amounts of cellular carbon and nitrogen, the balance between them, in term of C/N ratio, critically affect plant growth and development[4,5].

To clarify the molecular mechanism of plant C/N response, our laboratory had carried out mutant screening and had identified a plant specific RING-type E3 ubiquitin ligase CNI1/ATL31 as a C/N regulator in *Arabidopsis*. Overexpression of *ATL31* gene results in plants insensitive to disrupted high C/low N stress condition, in which wild-type plant showed severe growth arrest and anthocyanin accumulation at the post-germinative checkpoint[6]. Subsequent study revealed that ATL31 directly interacts with and regulates the stability of 14-3-3 proteins by ubiquitination followed by proteasomal degradation in response to C/N condition[7,8]. Besides ATL31, using same screening method, I identified an additional mutant, *cni2-D (carbon/nitrogen insensitive 2-dominant)*, showed the insensitive phenotype similar to *ATL31* overexpressors in C/N stress condition. The following analysis revealed that *ABI1* gene was over-expressed in *cni2-D* mutant. ABI1 is a phosphatase belongs to PP2C protein family, negatively regulates plant hormone abscisic acid (ABA) signaling pathway via directly dephosphorylation and inactivation of the downstream SnRK2 kinase. In Chapter I, I demonstrated that ABI1 regulates plant C/N response via a non-canonical ABA signaling pathway independently on ABA biosynthesis. I also discussed recently advanced research which revealed direct crosstalk between ABA signaling and other environmental signaling pathways in plant cells.

As well as vegetative growth, reproductive fruit development also highly relies on nutrient availabilities especially carbon and nitrogen[9]. To address the importance of carbon and nitrogen in the regulation of fruit development, I characterized and analyzed C/N regulators, ATL31 and 14-3-3, in tomato fruit (*Solanum lycopersicum* L.). 14-3-3 proteins are highly conserved versatile regulators that interact with phosphorylated clients and regulate their functions[10,11,12]. The lacking of information of ATL31 and 14-3-3 targets in tomato fruits inspired us to characterized tomato SlATL31 and identified 14-3-3 clients in tomato fruits for the indirectly understanding of the C/N nutrient significance in tomato fruit development, which details was described in Chapter II.

1. Krouk, G. *et al.* Nitrate-regulated auxin transport by NRT1.1 defines a mechanism for nutrient sensing in plants. *Dev. Cell* **18,** 927–37 (2010).
2. Smeekens, S., Ma, J., Hanson, J. & Rolland, F. Sugar signals and molecular networks controlling plant growth. *Curr. Opin. Plant Biol.* **13,** 274–9 (2010).
3. Stitt, M., Lunn, J. & Usadel, B. Arabidopsis and primary photosynthetic metabolism - more than the icing on the cake. *Plant J.* **61,** 1067–91 (2010).
4. Coruzzi, G. M. & Zhou, L. Carbon and nitrogen sensing and signaling in plants: emerging 'matrix effects'. *Curr. Opin. Plant Biol.* **4,** 247–53 (2001).
5. Martin, T., Oswald, O. & Graham, I. A. Arabidopsis seedling growth, storage lipid mobilization, and photosynthetic gene expression are regulated by carbon:nitrogen availability. *Plant Physiol.* **128,** 472–81 (2002).
6. Sato, T. *et al.* CNI1/ATL31, a RING-type ubiquitin ligase that functions in the carbon/nitrogen response for growth phase transition in Arabidopsis seedlings. *Plant J.* **60,** 852–64 (2009).
7. Sato, T. *et al.* Identification of 14-3-3 proteins as a target of ATL31 ubiquitin ligase, a regulator of the C/N response in Arabidopsis. *Plant J.* **68,** 137–46 (2011).
8. Yasuda, S. *et al.* Phosphorylation of arabidopsis ubiquitin ligase ATL31 is critical for plant carbon/nitrogen nutrient balance response and controls the stability of 14-3-3 proteins. *J. Biol. Chem.* **289,** 15179–15193 (2014).
9. Pate, J. S., Sharkey, P. J. & Atkins, C. A. Nutrition of a developing legume fruit: functional economy in terms of carbon, nitrogen, water. *Plant Physiol.* **59,** 506–10 (1977).
10. Obsil, T. & Obsilova, V. Structural basis of 14-3-3 protein functions. *Semin. Cell Dev. Biol.* **22,** 663–72 (2011).
11. Roberts, M. R. 14-3-3 Proteins find new partners in plant cell signalling. *Trends Plant Sci.* **8,** 218–223 (2003).
12. Chevalier, D., Morris, E. R. & Walker, J. C. 14-3-3 and FHA domains mediate phosphoprotein interactions. *Annu. Rev. Plant Biol.* **60,** 67–91 (2009).

CHAPTER I

ABI1 regulates carbon/nitrogen-nutrient signal transduction independent of ABA biosynthesis and canonical ABA signalling pathways in *Arabidopsis*

Summary

Plants are able to sense and mediate the balance between carbon (C) and nitrogen (N) nutrient availability to optimize metabolism and growth, described as the C/N response. To clarify the C/N signaling mechanism, C/N insensitive plant were obtained from Arabidopsis FOX hunting population, which overexpresses full-length cDNAs for individuals. The resulting *cni2-D* (*carbon/nitrogen insensitive 2-dominant*) plant was found to overcome the post-germinative growth checkpoint and expand green cotyledons in disrupted high C/low N stress condition. The *CNI2* gene encodes ABI1, a phosphatase type 2C protein, which negatively regulates abscisic acid (ABA) signal transduction. Overexpressors of *ABI1* were found to be insensitive to disrupted C/N stress, whereas the loss-of-function mutant *abi1-2* was hypersensitive, suggesting that ABI1 plays an essential role in plant C/N response. In contrast, the C/N-dependent growth phenotype observed in wild-type plants was not associated with endogenous ABA contents. Accordingly, the ABA insensitive mutant *abi1-1*, which could not bind to ABA-ABA receptor complex, was not insensitive and restored normal sensitivity to high C/low N stress. The canonical ABA signaling mutants *abi4* and *abi5* were also sensitive to disrupted C/N stress. Further gene expression analysis demonstrated that several genes in the SnRK2s and SnRK1s pathways are transcriptionally affected by high C/low N stress in wild-type plants regardless of the lack of increased endogenous ABA contents, whereas the expression of these genes were significantly suppressed in ABI1 over-expressors. Taken together, these results suggest direct crosstalk between C/N and non-canonical ABA signaling pathways, regulated by ABI1, in plants.

Introduction

Plant growth and development are controlled by many environmental factors and stresses, including nutrition, light, drought, and osmotic stress. Carbon and nitrogen are essential for plants, being constituents of nutrients and metabolites that provide energy and serve as constitutive molecular backbones. Moreover , these constitutive molecules also possess hormone-like functions, transducing signals to regulate plant growth and development[1,2,3]. In addition to absolute amounts of cellular carbon (C) and nitrogen (N), the relative C/N balance has been found to critically affect plant growth and development[4,5,6]. Several genome-wide investigations have shown that carbon and nitrogen metabolites and signaling cooperatively control various pathways involved in plant growth and development, such as glycolysis/gluconeogenesis, the pentose-phosphate pathway, protein synthesis, protein degradation, protein targeting and regulation of protein activity[7,8]. Despite the physiological importance of the C/N response, molecular mechanisms mediated by C/N signals remain unclear.

To assess the molecular mechanisms mediating plant C/N responses, I screened transgenic plants for novel gain-of-function using the *Arabidopsis* FOX (Full-length cDNA Over-eXpressing) hunting system, which consists of independent transgenic lines expressing full-length cDNAs under control of the CaMV promoter[9]. Previously researcher in my lab isolated a novel C/N insensitive mutant, called *carbon/nitrogen insensitive 1-D* (*cni1-D*) plants, and found that the *CNI1* gene encoded the ubiquitin ligase ATL31[6]. Overexpression of *ATL31* rescued plants from the post-germinative development arrest under extremely high C/low N stress conditions[6]. Subsequent analysis showed that ATL31 interacts with and ubiquitinates 14-3-3 and regulates plant growth via 14-3-3 degradation in response to C/N status[10].

The phytohormone abscisic acid (ABA) is critical for plant growth in response to environment challenges, such as drought, salt, and osmotic stress. Additional exogenous ABA delaying germination and arresting plant growth, similar to plants exposed to excess sugar stress[11,12]. Genetic approaches have identified several sugar insensitive mutants[13,14], with many of these mutants found to be defective in ABA biosynthesis or ABA signaling, include *gin1*/*ABA2*[15], *gin5*/*ABA3*[16] and *sun6*/*ABI4*[17]. These findings showed close positive interactions between sugar and ABA signaling.

Although sugar-ABA response has been thoroughly investigated[18,19,20], the relationship between C/N stress and ABA signaling has not yet been clarified.

To further assess the molecular mechanisms involved in C/N signaling in higher plants, I screened C/N response mutants and isolated a novel FOX transgenic plant, *cni2-D* (*carbon/nitrogen insensitive 2-dominant*), which was able to survive under extremely high C/low N stress conditions. The *CNI2* gene encodes a type 2C protein phosphatase, ABI1, a negative regulator of ABA signaling. ABI1 is a central component of ABA signaling transduction, with its phosphatase activity inhibiting several SnRK2 proteins[11,21]. ABA and the ABA-receptor complex bind to ABI1 and inhibit its function when ABA is present[22], resulting in the activation of SnRK2s kinase activity and ABA signal transduction.

This study investigated the physiological function of ABI1 at the post-germinative growth checkpoint in response to C/N, demonstrating that ABI1 negatively regulates C/N signaling. In contrast, quantification of ABA amounts and genetic analysis demonstrated that C/N signaling is not mediated via ABA biosynthesis and the canonical ABA signaling pathway that regulates sugar signaling through ABI4 and ABI5. These results provide new insight into the cross-talk between C and N signaling and its effect on the non-canonical ABA signaling pathway under the control of ABI1 protein.

Materials and methods

Plant materials and growth conditions

Wild-type *Arabidopsis thaliana* Columbia-0 (Col-0) and all other plant materials used in this study were grown under previously described conditions[6]. The Arabidopsis FOX hunting population was provided by RIKEN[9]. The ABA insensitive mutants *abi1-1*[23,24], *abi1-2* (SALK_072009)[25], *abi4-102* (CS3837)[15], and *abi5-1* (line ID:CS8105)[26] were obtained from the Arabidopsis Biological Resource Center (Ohio State University, OH, USA). Surface-sterilized seeds were plated on modified MS medium. After stratification for 3-days at 4^{o}C in the dark, the plates were incubated at 22^{o}C with a 16-h light/8-h dark cycle.

Isolation of the cni2-D plant

The *cni2-D* plant was isolated by screening Arabidopsis FOX lines with selection medium containing 300 mM glucose and 0.1 mM nitrogen as described previously[6]. The identity of the *ABI1* gene was determined by PCR using T-DNA primers that amplify the inserted cDNA fragment[9]. The resulting PCR fragments were cloned into the pCR2.1 vector (Invitrogen, http://www.invitrogen.com) and sequenced.

C/N response assay

Surface-sterilized seeds were sown on MS medium modified with different concentrations of glucose and total nitrogen, as described[6]. The number of green-colored cotyledons was counted 7-days after sowing. For transient limited-nitrogen treatment, seedlings were transferred to medium containing 0.3 mM nitrogen after being grown for 7 days in control medium containing 3 mM nitrogen.

Plasmid constructions and plant transformation

Full-length *ABI1* cDNA fragment was amplified by PCR using the primers described in Table 1. The fragment was sequenced and cloned into the pENTR/D-TOPO vector (Invitrogen) to generate the plasmid pENTR/ABI1. Full-length *ABI1* cDNA was subsequently introduced into the pMDC83 T-DNA binary vector[27], according to the Gateway instruction manual (Invitrogen), placing the full-length *ABI1* gene under control of the 35S promoter (*35S-ABI1*). This *35S-ABI1* construct was used to transform Arabidopsis as described[6].

Transcript level analysis

Total RNA was isolated from plants as described[6], and 500 ng RNA were reverse transcribed to cDNA with Super Script II (Invitrogen). RT-PCR analysis was performed with normalized cDNA samples for appropriate cycles, using the primer sets described in Table 2. PCR products were electrophoresed on agarose gel and visualized by ethidium bromide staining. Quantitative RT-PCR (qRT-PCR) was performed using SYBR premix EX Taq (TAKARA) on an Mx3000P QPCR System (Agilent Technologies)

according to the manufacturer's protocol. The internal control for calculating ΔΔCt was *18S rRNA*. The specific primer sets used for qRT-PCR analysis are shown in Table 2.

Quantitative analysis of endogenous ABA content

The ABA contents of Arabidopsis plantlets were analyzed essentially as described[28]. Briefly, plantlets were grown for 7 days after germination in each C/N medium. Approximately 100 mg of fresh weight of each were frozen in liquid nitrogen and ground into fine powder by vigorously shaking with a vortex mixer in a 14 mL round bottom plastic tube together with a 10-mm Zirconia bead. ABA was extracted twice with 4 mL of 80% (v/v) acetonitrile containing 1% (v/v) acetic acid and the internal standard (4 ng d_6-ABA, Icon Isotopes, Summit, NJ, USA) at 4°C for 1 h. After clearing by centrifugation, the supernatant was evaporated and loaded onto an Oasis HLB column (Waters, Milford, MA, USA). The eluate containing ABA was evaporated and applied to an Oasis MCX column (Waters) to remove cationic compounds. After washing the column with 1% acetic acid, ABA was eluted with 80% acetonitrile containing 1% acetic acid. The eluate was evaporated and applied to an Osasis WAX column (Waters). After successive washes with 1% acetic acid and 80% acetonitrile, the acidic fraction containing ABA was eluted with 80% acetonitrile containing 1% acetic acid. This fraction was dried and dissolved in 1% acetic acid. ABA was determined by LC-MS/MS (Agilent 6410) using a ZORBAX Eclipse XDB-C18 column (Agilent).

Results

Isolation of cni2-D transgenic plant able to tolerate C/N stress condition

To assess the molecular mechanisms involved in plant C/N response, FOX hunting populations were screened using medium containing an extremely high concentration of glucose (300 mM Glc) and limited nitrogen (0.1 mM N), termed high C/low N condition. This screening resulted in the identification of a new C/N response mutant, *carbon/nitrogen insensitive 2-D* (*cni2-D*), which could continue post-germinative growth, in the extremely high C/low N medium (Fig. 1A). Under this condition, wild-type (WT) plant showed severe growth defect and strong purple accumulation of anthocyanin,

whereas *cni2-D* plant could grow and generate green cotyledons. The full-length cDNA fragment inserted in the *cni2-D* FOX plant was recovered by genomic PCR using primers complementing the T-DNA construct. Sequencing of the recovered cDNA identified *At4g26080* as the *CNI2* gene, which encodes the protein ABI1, a Ser/Thr phosphatase type 2C (PP2C). This protein has been shown to negatively regulate ABA signaling by inhibiting downstream SnRK2s kinase activities[29,30]. Genomic PCR and RT-PCR analyses confirmed that full length cDNA of ABI1 had been inserted into and overexpressed in *cni2-D* plant (Fig. 1B).

Over-expression of ABI1 gene causes C/N stress insensitivity seen in cni2-D plant

To further confirm that the *ABI1* gene was responsible for the *cni2-D* phenotype, transgenic *Arabidopsis* plants over-expressing *ABI1* under control of CaMV 35S promoter (*35S-ABI1*) were grown in C/N stress medium. The transgenic nature of these plants was confirmed by genomic PCR and RT-PCR analyses (Fig. 1C). C/N response analysis was assessed in these plants grown under relatively mild high C/low N stress condition (200 mM Glc/0.3 mM N), since the screening medium (300 mM Glc/0.1 mM N) was too severe for further analysis. Seeds of WT and *35S-ABI1* plants were sown in normal (100 mM Glc/3 mM N) and high C/low N stress (200 mM Glc/0.3 mM N) media. Although WT plants showed growth defects in this C/N stress medium, *35S-ABI1* plants expanded green cotyledons and continued post-germinative growth (Fig. 1D and Fig. 2).

The transcript levels of marker genes responsible for the C/N response were analyzed. In WT plants, the expression level of the photosynthesis-related *RBCS1-B* gene was lower in high C/low N stress condition than in normal condition, whereas expression of this gene in *35S-ABI1* plants was equal under both conditions (Fig. 1E). In contrast, the induction of the anthocyanin biosynthesis genes *PAP1* and *CHS* under high C/low N stress condition was suppressed in *35S-ABI1* plants (Fig. 1E). These results demonstrate that overexpression of the *ABI1* gene causes the *cni2-D* phenotype, which is resistant to high C/low N stress.

Over-expressor and loss-of-function mutant of ABI1 gene show reciprocal phenotypes under C/N stress condition

To further evaluate the function of ABI1 in plant C/N response, growth of the *35S-ABI1* and the loss-of-function mutant *abi1-2* was examined in parallel under several C/N stress conditions. Seeds of WT plants and *35S-ABI1* and *abi1-2* mutants were grown at constant nitrogen concentration (0.3 mM) with various glucose concentrations (0, 100, and 200 mM) and at constant glucose concentration (200 mM) with various nitrogen concentrations (0.3, 1 and 3 mM). Almost all WT, *35S-ABI1* and *abi1-2* plants grew normally and expanded green-colored cotyledons in 0 mM Glc/0.3 mM N medium (Fig. 3A). The post-germinative growth of WT plants was inhibited and the number of individuals expanded green cotyledons reduced to 22% in 100 mM Glc/0.3 mM N medium (Figs. 3A and 3C). WT plants growth was more severely inhibited and less than 5% WT plants showed green cotyledons expansion in 200 mM Glc/0.3 mM N medium. In contrast, the greening ratio of *35S-ABI1* plants was 52% in 100 mM Glc/0.3 mM N and 32% in 200 mM Glc/0.3 mM N (Figs. 3A and 3C), indicating that these plants were insensitive to increased glucose when nitrogen was limited. In contrast, growth inhibition was enhanced in *abi1-2* mutants, with the greening ratio decreased to 6% in 100 mM Glc/0.3 mM N and 0% in 200 mM Glc/0.3 mM N (Figs. 3A and 3C). The growth inhibitory due to increased Glc was not due to osmotic stress, because the WT and *abi1-2* plants did not show anthocyanin accumulation or growth defects in media containing 0.3 mM N with 100 or 200 mM mannitol (Fig. 4).

The effects of exogenous nitrogen availability on these mutants were examined in the presence of a constant sugar amounts. Although most WT, *35S-ABI1* and *abi1-2* plants could grow normally and expanded green cotyledons in 200 mM Glc/3 mM N medium, WT plant growth was relatively inhibited and showed decreased greening ratio (30%) in 200 mM Glc/1 mM N. This inhibition was more apparent in the *abi1-2* mutant (11%), while *35S-ABI1* plants were insensitive (78%) (Figs. 3B and 3D). Severe growth defects of WT and *abi1-2* mutants were observed in 200 mM Glc/0.3 mM N, while *35S-ABI1* was insensitive. Taken together, these results clearly demonstrate the reciprocal phenotypes of *35S-ABI* and *abi1-2* in response to increased Glc and limited N availability in the medium, suggesting that ABI1 plays an essential role in regulating plant growth in response to C/N status.

ABA biosynthesis is not associated with plant growth defect in response to C/N status

ABI1 is a phosphatase that is directly repressed by interaction with the ABA receptor PYR/RCAR in the presence of ABA, resulting in activation of ABA signaling. Endogenous amounts of ABA have been reported increased by excess sugar in the medium, leading to growth arrest of Arabidopsis seedlings and indicating that endogenous sugar levels positively affect ABA biosynthesis. However the relationship between C/N availability and ABA biosynthesis has not been determined. To determine whether the C/N-induced growth defect is caused by increased ABA level, endogenous ABA contents were measured in WT Arabidopsis seedlings grown under each C/N conditions. WT seedlings were grown in medium containing different concentrations of glucose (0, 100, 200 and 300 mM) and nitrogen (0.3, 1, 3 mM) for 7 days (Fig. 5A) and ABA amounts quantified by LC-MS analysis. ABA content was 5 ng/mg FW in seedlings grown in 0 mM Glc/3 mM N and was significantly increased to 12, 20 and 63 ng/mg FW during growth in medium containing 0.3 mM N with 50, 100 and 200 mM glucose, respectively (Fig. 5B). Similar Glc-dependent increases in ABA contents were observed at all N concentrations, although the effects were lower at lower N concentrations (Fig. 5B). Surprisingly, ABA contents were decreased in response to limited N. In the presence of 100 mM glucose, ABA contents were estimated to be 20, 15 and 10 ng/mg FW in seedlings grown in the presence of 3, 1 and 0.3 mM N, respectively. Similar patterns were observed in other N-modified media containing 50 mM and 200 mM Glc. Interestingly, the ABA contents of seedlings grown in 100 mM Glc/3 mM N and 200 mM Glc/0.3 mM N were similar (Fig. 5B), despite their growth phenotypes being totally different (Fig. 5A).

To confirm that nitrogen limitation directly affects ABA biosynthesis, I transferred WT plants grown in control medium (100 mM Glc/3 mM N) for 7 days to N-deficient medium (100 mM Glc/0.3 mM N). After 3-days, the ABA content of plants grown in N-deficient medium was slightly but significantly lower than that of control condition (Fig. 6A), similar to the results observed at stable low N (Fig. 5B). Transfer to N-deficient medium also increased the expression of *Gln1.4* mRNA, which encodes a cytosolic glutamine synthase, a typical marker induced by N starvation, confirming that the endogenous N level of plants was limited (Fig. 6B). In contrast, the level of *NCED3*

mRNA, which encodes a key enzyme for ABA biosynthesis, was not altered after the transfer (Fig. 6B). These results indicate that the growth defect observed in high C/low N stress medium is not due to increased ABA content, suggesting that more complex regulatory mechanisms are involved under ABI1 control to mediate C/N conditions.

ABA insensitive mutants, abi1-1, abi4 and abi5, are not insensitive to C/N stress condition

Since the C/N stress response phenotype did not associate with endogenous ABA content, then C/N response in *abi1-1* mutant was examined. In *abi1-1*, the Gly180 residue is replaced by Asp, with the mutated ABI1 protein unable to bind to the ABA-receptor complex, resulting in constitutive inactivation of SnRK2 proteins[31]. Thus, the *abi1-1* mutant was not insensitive to C/N stress and exhibited growth inhibition with anthocyanin accumulation, similar to WT plants (Fig. 7A). This result also suggests that the C/N response mediated by ABI1 is independent of ABA biosynthesis and is likely regulated by an alternative signaling cascade unlike typical ABA signaling cascades. To evaluate the C/N-responsive signaling pathway associated with ABI1, I tested the C/N responses of *abi4* (*abi4-102*) and *abi5* (*abi5-1*) loss-of-function mutants, since these genes encode key canonical transcriptional factors under the control of ABI1-SnRK2s[29]. My colleagues had previously shown that these *abi4* and *abi5* mutants are not resistant to the extremely high C/low N stress condition (300 mM G/0.1 mM N) used in *cni* mutant screening[6]. I, therefore, re-examined the detailed C/N responses of these mutant to relatively milder high C/low N stress conditions (200 mM Glc/0.3 mM N) and quantified the ratio of green-colored cotyledons. Both *abi4* and *abi5* mutants were sensitive to C/N stress, with both having similar greening ratios to WT plants (Figs. 7B and 7C) and the *abi1-1* mutant (Fig. 7A).

These results strongly suggested that ABI1 controls plant C/N responses, but that these responses are mediated through a non-canonical typical ABA signaling pathway such as ABI4 and/or ABI5.

Expression of ABA-related marker genes is differentially affected in response to C/N and is controlled by ABI1 regulation

To assess the C/N-mediated signal transduction pathway under ABI1 control, transcript analysis was performed in WT and *ABI1* over-expressor (*35S-ABI1*) plants. The expression of *CHS* was about 13-fold higher in WT plants grown under high C/low N stress (200 mM Glc/0.3 mM N) than under control (100 mM Glc/3 mM N) condition, whereas *CHS* induction was clearly suppressed in *35S-ABI1* plants (Fig. 8A), confirming that ABI1 functions in C/N response. Moreover, the expression of *NCED3*, which encodes an ABA-biosynthetic enzyme, was not increased by high C/low N stress in WT plants (Fig. 8B), a finding consistent with the results of ABA quantification (Fig. 5B). The expression of *NCED3* was slightly higher in *35S-ABI1* than in WT plants, suggesting that ABA content is not responsible for the insensitive phenotype of *35S-ABI1* plants under high C/low N stress condition. Evaluation of the expression of several ABA-responsive marker genes in the SnRK2s pathway[32] showed that *RD29b* expression in WT plants was about 6-fold higher under high C/low N stress than under control conditions, but that *RD29b* expression was slightly lower in *35S-ABI1* plants under stress conditions (Fig. 8C). Similar expression patterns were observed for the *LEA3-4* and *TSPO* genes (Figs. 8D and 8E). In contrast, the levels of expression of *RAB18*, *AREB1* and *ABF3* were not increased by high C/low N stress and were similar in WT and *35S-ABI1* plants (Figs. 8F-8H). These results suggested that C/N stress activates some, but not all, of the ABA signaling cascade involving SnRk2s. I also evaluated SnRK1s-regulated marker genes, such as *DIN6* and *SEN5*[33,34], since SnRK1s are important for energy homeostasis and recently reported to be direct targets of ABI1[34]. Transcript analyses showed that the levels of expressions of *DIN6* and *SEN5* in WT plants were significantly decreased in response to high C/low N stress, but were not affected in *35S-ABI1* plants (Fig. 8I and 8J). Taken together, these results suggest that high C/low N stress affects specific ABA-related signal transduction cascades under the control not only of SnRk2s but also of SnRK1s, and is independent of ABA biosynthesis.

Discussion

Identification of ABI1 as a C/N-response regulator

The *cni2-D* plants isolated in this study were insensitive to disrupted C/N-nutrient stress condition, with *ABI1* being responsible gene for the phenotype of these plants

(Fig. 1). Overexpression of *ABI1* caused the successful post-germinative growth of these plants under high C/low N stress condition, while the loss-of-function mutants showed hyper-sensitive responses and severe growth inhibition when compared with WT plants (Fig. 3), clearly demonstrating the importance of ABI1 plays in C/N signal regulation in Arabidopsis. *ABI1* encodes a protein phosphatase and functions as an essential negative regulator of ABA signal transduction. It has been reported that ABA is involved in multiple stress signal mediations including the sugar and osmotic signals during post-germination growth. Sugar and osmotic stresses enhances ABA biosynthesis followed by inhibition of ABI1 and then activation of ABA signaling cascade[35,36,37]. Interestingly, however, ABA quantification analysis showed that endogenous ABA content is not correlated with growth inhibition in response to C/N status (Fig. 5). This finding was consistent with results showing that the *abi1-1* mutant, in which mutated ABI1 is unable to bind to the ABA-receptor complex, resulting in the constitutive inactivation of SnRK2s, was not resistant to C/N stress (Fig. 7). In addition, loss-of-function mutants of *ABI4* and *ABI5* were not insensitive to high C/low N stress condition (Fig. 7), despite being resistant to high sugar stress and exogenous ABA at normal N concentration[38]. These results indicated that high C/low N stress treatment used in this study is distinguishable from osmotic stress and that the C/N signaling cascade is not redundant to the canonical sugar- and ABA-signaling pathway under ABI1 control.

ABA biosynthesis in response to N and C/N status

I found that ABA biosynthesis is affected by C/N status but is not associated with plant growth phenotype in response to C/N (Fig. 5). ABA content was not increased under high C/low N stress condition, although sugar promotes ABA biosynthesis. Both continuous and transient nitrogen limitation did not enhance the expression of *NCED3*, which encodes a key enzyme in ABA biosynthesis, under both high C/low N and limited-N conditions (Figs. 6 and 8).

Since little was known about the relationship between ABA biosynthesis and nitrogen availability, the results of this study are complicated. Related studies have reported that ABA biosynthesis in aerial parts of cucumbers is affected by limited

nitrogen, but that this effect is dependent on time after treatment and developmental stage[39]. In Arabidopsis, transcription analysis showed that the expression of ABA biosynthetic genes could be activated by nitrogen starvation as well as by sugar supplementation[40]. In contrast, the ABA contents of shoot and root were similar in Arabidopsis plants grown at high and low nitrogen conditions[41]. Thus the effect of nitrogen on ABA biosynthesis may depend on developmental stage, N-treatment condition and plant species, suggesting that a complex system regulates ABA biosynthesis in response to nitrogen availability. Although the direct participation of the ABA signaling pathway in nitrogen signal mediation remains unclear, genetic studies have demonstrated that the ABA pathway is involved in regulating plant development in response to nitrogen status. ABA-insensitive mutants such as *abi4* and *abi5* and ABA-deficient mutants were shown to be less sensitive to the inhibitory effects of high nitrate medium on lateral root formation[42]. Further studies are needed to determine the physiological function of the ABA pathway in mediating nitrogen availability and disrupted C/N stress.

C/N signaling cascade under ABI1 control

The results in this study raise the question about how ABI1 regulates post-germinative growth in response to C/N. To explore the unknown signaling pathway mediated by C/N response under ABI1 control, I examined transcript levels of several ABA-signaling marker genes regulated by the SnRK2s pathway. Interestingly, although endogenous ABA contents were not up-regulated, the levels of expression of *RD29b*, *LEA3-4*, *TSPO* were increased by high C/low N stress, and suppressed in *ABI1* overexpressing plants (Fig. 8), suggesting a direct crosstalk between C/N and the ABA signaling pathway under ABI1 control. On the other hands, the levels of expressions of other marker genes, *RAB18*, *AREB1* and *ABF3*, were not affected by high C/low N stress, indicating that C/N signals are mediated by specific ABA signaling pathways. Additionally, I investigated the involvement of the SnRK1s, a family of essential kinases associated with vast transcriptional events and metabolic reprogramming, restoring homeostasis and inducing tolerance to energy starvation stress[43,44]. Recent studies showed that besides SnRK2s, ABI1 could directly target also SnRK1s[34] and SnRK1s is

involved in ABA signaling[35]. My transcript analyses demonstrated that high C/low N stress decreased the expression of *DIN6* and *SEN5*, both of which are typical SnRK1s-responsive marker genes, in WT plants, but which effect was clearly suppressed in *ABI1* over-expressor (Fig. 8). This finding suggests the importance of the SnRK1s pathway in C/N signal mediation under ABI1 control. In responding to cellular energy status, SnRK1s target key components involved in protein synthesis and autophagic degradation[1]. Moreover, SnRK1s proteins have been reported to phosphorylate various 14-3-3 targeting proteins involved in primary carbon and nitrogen metabolism, including nitrate reductase (NR) and sucrose 6-phosphate synthase (SPS)[45,1], suggesting a strong relationship to C/N response. Previous study revealed that 14-3-3 is targeted by ATL31 for ubiquitination and is essential for post-germinative growth regulation in response to C/N[10]. Alternatively, a proteomics analysis showed that SPS enzyme was precipitated along with ABI1 protein[46], suggesting that ABI1 may regulate metabolic enzyme activity. Further biochemical and genetic analyses are required to understand the detailed functions of ABI1 and downstream SnRK proteins in plant C/N response.

Direct interaction between ABA signal and other cellular signaling pathway

The ABA receptors PYRs/PYLs/RCARs, PP2Cs and SnRK2s constitute the core signal transduction system that regulates plant growth in response to environmental stimuli, with this regulation being highly dependent on the presence or absence of ABA. In addition to ABA, several abiotic stresses were found to modulate PP2Cs and SnRK2s signaling activity, similarly to my finding that C/N-nutrient stress could activate specific ABA signaling pathways independent of ABA biosynthesis. Here I summarize several reports describing the alternative regulation of PP2Cs and SnRK2s function independent of ABA biosynthesis and perception (Table 3).

Reactive oxygen species (ROS) are key secondary messengers that respond to a variety of stress conditions. Hydrogen peroxide is the major ROS produced by plants. Recently, hydrogen peroxide was found to inhibit the activity of HOMOLOGY TO ABI1 (HAB1), a PP2C protein involved in ABA signaling in Arabidopsis[47]. Hydrogen peroxide promotes the dimerization of HAB1 and blocks the interactions between HAB1 and downstream SnRK2s by oxidizing the Cys-186 and Cys-247 residues of HAB1. These

findings demonstrated that hydrogen peroxide regulates PP2C activities and mediates ABA signaling. Although ABA promotes the production of hydrogen peroxide, the inhibition of PP2C by hydrogen peroxide can occur in the absence of ABA and ABA receptor[47], suggesting that ABA signaling is directly regulated by hydrogen peroxide produced by other signaling cascades.

ROPs are plant specific Rho-like small GTPase family proteins, with their activity dependent on alternative binding to GTP or GDP. Arabidopsis ROP11 negatively regulates ABA mediated stomatal closure, seed germination, post-germinative growth and ABA marker gene expression by interacting with and protecting ABI1 phosphatase activity[48,49].

It had been proposed that SnRK2s activities are regulated by osmotic stress both of ABA-dependent and -independent manner. Arabidopsis SnRK2.6/OST1, a member of the SnRK2 group III subfamily, is activated in response to osmotic stress via its C-terminal domain 2 in an ABA independent manner[50]. SnRK2s are activated even in ABA-deficient and ABA-insensitive mutants subjected to osmotic stress, and may be activated by an upstream kinase rather than conventional auto-activation[51]. The ABA independent osmotic stress response and the ABA independent kinase pathway via SnRK2s and their downstream transcriptional factors have been thoroughly reviewed[52,53].

Direct crosstalk between ABA and brassionsteroid (BR) has also been reported. Arabidopsis BRASSINOSTEROID INSENSITIVE2 (BIN2) kinase, a negative regulator of BR signaling in Arabidopsis plants, and its homologues BIN2-LIKE1 (BIL1) and BIL2, directly interact with ABI5 transcription factor in the nucleus[54]. ABI5 phosphorylation by BIN2 and its homologues stabilizes ABI5 protein, enhancing ABA signaling and inhibiting germination and post-germinative growth. BIN2 and its homologues also directly interact with and phosphorylate SnRK2.2 and SnRK2.3, activating downstream ABA signaling and inhibiting root elongation[55].

SnRK2.6/OST1 is predominantly expressed in guard cells and contributes to the global regulation of ABA-associated stomatal closure by auto-phosphorylation in the absence of inhibition by PP2C protein. However, the existence of an upstream kinase could not be ignored, since SnRK2.6/OST1 has been detected in other tissues and

plays potential role in processes other than ABA signaling, for example in sucrose metabolism[56]. The casein kinase 2 (CK2) holoenzyme complex, which is comprised of two α-catalytic subunits and two β-regulatory subunits, was recently shown to phosphorylate SnRK2.6/OST1 in maize[57]. This phosphorylation negatively regulates ABA signaling by enhancing the interaction between SnRK2.6/OST1 and PP2C and also promotes SnRK2.6/OST1 degradation via the 26S proteasome system[57]. These molecular findings demonstrate that additional upstream kinases could regulate SnRK2 activity as well as ABA signaling.

Nitric oxide (NO) is an important secondary messenger that regulates many aspects of plant responses, including ABA-induced stomatal closure[58,59]. The NO dependent S-nitrosylation of SnRK2.6/OST1 at the Cys-137 residue was recently shown to negatively regulate SnRK2.6/OST1 activity and ABA mediated stomatal closure in Arabidopsis[60]. NO accumulates in mutants lacking the S-nitrosoglutathione reductase (GSNOR) gene, resulting in impaired ABA inducible stomatal closure. Interestingly, a cysteine residue corresponding to Cys137 of SnRK2.6 is present in several yeast and human protein kinases and could be S-nitrosylated, suggesting that S-nitrosylation may be an evolutionarily conserved mechanism for regulating protein kinases[60].

In addition to my finding, that C/N signals are mediated via a non-canonical ABA signaling pathway, several studies have shown crosstalk between ABA signal transduction and multiple cellular signals, suggesting that multiple environmental signals are integrated into the ABA signaling cascade. Further studies will reveal the detailed molecular basis and physiological significance of this integration mechanism, optimizing plant growth in nature.

Reference

1. Smeekens, S., Ma, J., Hanson, J. & Rolland, F. Sugar signals and molecular networks controlling plant growth. *Curr. Opin. Plant Biol.* **13,** 274–9 (2010).
2. Krouk, G., Crawford, N. M., Coruzzi, G. M. & Tsay, Y.-F. Nitrate signaling: adaptation to fluctuating environments. *Curr. Opin. Plant Biol.* **13,** 266–73 (2010).
3. Stitt, M., Lunn, J. & Usadel, B. Arabidopsis and primary photosynthetic metabolism - more than the icing on the cake. *Plant J.* **61,** 1067–91 (2010).
4. Martin, T., Oswald, O. & Graham, I. A. Arabidopsis seedling growth, storage lipid mobilization, and photosynthetic gene expression are regulated by carbon:nitrogen availability. *Plant Physiol.* **128,** 472–81 (2002).
5. Coruzzi, G. M. & Zhou, L. Carbon and nitrogen sensing and signaling in plants: emerging 'matrix effects'. *Curr. Opin. Plant Biol.* **4,** 247–53 (2001).
6. Sato, T. *et al.* CNI1/ATL31, a RING-type ubiquitin ligase that functions in the carbon/nitrogen response for growth phase transition in Arabidopsis seedlings. *Plant J.* **60,** 852–64 (2009).
7. Gutiérrez, R. a *et al.* Qualitative network models and genome-wide expression data define carbon/nitrogen-responsive molecular machines in Arabidopsis. *Genome Biol.* **8,** R7 (2007).
8. Palenchar, P. M., Kouranov, A., Lejay, L. V & Coruzzi, G. M. Genome-wide patterns of carbon and nitrogen regulation of gene expression validate the combined carbon and nitrogen (CN)-signaling hypothesis in plants. *Genome Biol.* **5,** R91 (2004).
9. Ichikawa, T. *et al.* The FOX hunting system: an alternative gain-of-function gene hunting technique. *Plant J.* **48,** 974–85 (2006).
10. Sato, T. *et al.* Identification of 14-3-3 proteins as a target of ATL31 ubiquitin ligase, a regulator of the C/N response in Arabidopsis. *Plant J.* **68,** 137–46 (2011).
11. Umezawa, T. *et al.* Type 2C protein phosphatases directly regulate abscisic acid-activated protein kinases in Arabidopsis. *Proc. Natl. Acad. Sci. U. S. A.* **106,** 17588–93 (2009).
12. Dekkers, B. J. W., Schuurmans, J. a M. J. & Smeekens, S. C. M. Interaction between sugar and abscisic acid signalling during early seedling development in

Arabidopsis. *Plant Mol. Biol.* **67,** 151–67 (2008).

13. Smeekens, S. SUGAR-INDUCED SIGNAL TRANSDUCTION IN PLANTS. *Annu. Rev. Plant Physiol. Plant Mol. Biol.* **51,** 49–81 (2000).
14. Rook, F. & Bevan, M. W. Genetic approaches to understanding sugar-response pathways. *J. Exp. Bot.* **54,** 495–501 (2003).
15. Laby, R. J., Kincaid, M. S., Kim, D. & Gibson, S. I. The Arabidopsis sugar-insensitive mutants sis4 and sis5 are defective in abscisic acid synthesis and response. *Plant J.* **23,** 587–96 (2000).
16. Rolland, F., Moore, B. & Sheen, J. Sugar sensing and signaling in plants. *Plant Cell* **14 Suppl,** S185-205 (2002).
17. Huijser, C. *et al.* The Arabidopsis SUCROSE UNCOUPLED-6 gene is identical to ABSCISIC ACID INSENSITIVE-4: involvement of abscisic acid in sugar responses. *Plant J.* **23,** 577–85 (2000).
18. Rolland, F., Baena-Gonzalez, E. & Sheen, J. Sugar sensing and signaling in plants: conserved and novel mechanisms. *Annu. Rev. Plant Biol.* **57,** 675–709 (2006).
19. Rook, F., Hadingham, S. a., Li, Y. & Bevan, M. W. Sugar and ABA response pathways and the control of gene expression. *Plant. Cell Environ.* **29,** 426–34 (2006).
20. Acevedo-Hernández, G. J., León, P. & Herrera-Estrella, L. R. Sugar and ABA responsiveness of a minimal RBCS light-responsive unit is mediated by direct binding of ABI4. *Plant J.* **43,** 506–19 (2005).
21. Vlad, F. *et al.* Protein phosphatases 2C regulate the activation of the Snf1-related kinase OST1 by abscisic acid in Arabidopsis. *Plant Cell* **21,** 3170–84 (2009).
22. Park, S.-Y. *et al.* Abscisic acid inhibits type 2C protein phosphatases via the PYR/PYL family of START proteins. *Science* **324,** 1068–71 (2009).
23. Leung, J. *et al.* Arabidopsis ABA response gene ABI1: features of a calcium-modulated protein phosphatase. *Science* **264,** 1448–52 (1994).
24. Meyer, K., Leube, M. P. & Grill, E. A protein phosphatase 2C involved in ABA signal transduction in Arabidopsis thaliana. *Science* **264,** 1452–5 (1994).
25. Saez, A. *et al.* Enhancement of abscisic acid sensitivity and reduction of water

consumption in Arabidopsis by combined inactivation of the protein phosphatases type 2C ABI1 and HAB1. *Plant Physiol.* **141,** 1389–99 (2006).

26. Finkelstein, R. R. Mutations at two new Arabidopsis ABA response loci are similar to the abi3 mutations. *Plant J.* **5,** 765–771 (1994).
27. Curtis, M. D. & Grossniklaus, U. A gateway cloning vector set for high-throughput functional analysis of genes in planta. *Plant Physiol.* **133,** 462–9 (2003).
28. Iehisa, J. C. M., Matsuura, T., Mori, I. C. & Takumi, S. Identification of quantitative trait locus for abscisic acid responsiveness on chromosome 5A and association with dehydration tolerance in common wheat seedlings. *J. Plant Physiol.* **171,** 25–34 (2014).
29. Raghavendra, A. S., Gonugunta, V. K., Christmann, A. & Grill, E. ABA perception and signalling. *Trends Plant Sci.* **15,** 395–401 (2010).
30. Umezawa, T. *et al.* Molecular basis of the core regulatory network in ABA responses: sensing, signaling and transport. *Plant Cell Physiol.* **51,** 1821–39 (2010).
31. Santiago, J. *et al.* Structural insights into PYR/PYL/RCAR ABA receptors and PP2Cs. *Plant Sci.* **182,** 3–11 (2012).
32. Mizoguchi, M. *et al.* Two closely related subclass II SnRK2 protein kinases cooperatively regulate drought-inducible gene expression. *Plant Cell Physiol.* **51,** 842–7 (2010).
33. Baena-González, E., Rolland, F., Thevelein, J. M. & Sheen, J. A central integrator of transcription networks in plant stress and energy signalling. *Nature* **448,** 938–42 (2007).
34. Rodrigues, A. *et al.* ABI1 and PP2CA phosphatases are negative regulators of Snf1-related protein kinase1 signaling in Arabidopsis. *Plant Cell* **25,** 3871–84 (2013).
35. Jossier, M. *et al.* SnRK1 (SNF1-related kinase 1) has a central role in sugar and ABA signalling in Arabidopsis thaliana. *Plant J.* **59,** 316–28 (2009).
36. León, P. & Sheen, J. Sugar and hormone connections. *Trends Plant Sci.* **8,** 110–6 (2003).
37. Fujii, H., Verslues, P. E. & Zhu, J.-K. Arabidopsis decuple mutant reveals the

importance of SnRK2 kinases in osmotic stress responses in vivo. *Proc. Natl. Acad. Sci. U. S. A.* **108,** 1717–22 (2011).

38. Arenas-Huertero, F., Arroyo, A., Zhou, L., Sheen, J. & León, P. Analysis of Arabidopsis glucose insensitive mutants, gin5 and gin6, reveals a central role of the plant hormone ABA in the regulation of plant vegetative development by sugar. *Genes Dev.* **14,** 2085–96 (2000).
39. Oka, M. *et al.* Abscisic acid substantially inhibits senescence of cucumber plants (Cucumis sativus) grown under low nitrogen conditions. *J. Plant Physiol.* **169,** 789–96 (2012).
40. Yang, Y., Yu, X., Song, L. & An, C. ABI4 activates DGAT1 expression in Arabidopsis seedlings during nitrogen deficiency. *Plant Physiol.* **156,** 873–83 (2011).
41. Kiba, T., Kudo, T., Kojima, M. & Sakakibara, H. Hormonal control of nitrogen acquisition: roles of auxin, abscisic acid, and cytokinin. *J. Exp. Bot.* **62,** 1399–409 (2011).
42. Signora, L., De Smet, I., Foyer, C. H. & Zhang, H. ABA plays a central role in mediating the regulatory effects of nitrate on root branching in Arabidopsis. *Plant J.* **28,** 655–662 (2002).
43. Baena-González, E. & Sheen, J. Convergent energy and stress signaling. *Trends Plant Sci.* **13,** 474–82 (2008).
44. Lunn, J. E., Delorge, I., Figueroa, C. M., Van Dijck, P. & Stitt, M. Trehalose metabolism in plants. *Plant J.* **79,** 544–67 (2014).
45. Comparot, S., Lingiah, G. & Martin, T. Function and specificity of 14-3-3 proteins in the regulation of carbohydrate and nitrogen metabolism. *J. Exp. Bot.* **54,** 595–604 (2003).
46. Nishimura, N. *et al.* PYR/PYL/RCAR family members are major in-vivo ABI1 protein phosphatase 2C-interacting proteins in Arabidopsis. *Plant J.* **61,** 290–9 (2010).
47. Sridharamurthy, M. *et al.* H2O2 inhibits ABA-signaling protein phosphatase HAB1. *PLoS One* **9,** e113643 (2014).
48. Li, Z., Kang, J., Sui, N. & Liu, D. ROP11 GTPase is a negative regulator of

multiple ABA responses in Arabidopsis. *J. Integr. Plant Biol.* **54,** 169–79 (2012).

49. Li, Z. *et al.* ROP11 GTPase negatively regulates ABA signaling by protecting ABI1 phosphatase activity from inhibition by the ABA receptor RCAR1/PYL9 in Arabidopsis. *J. Integr. Plant Biol.* **54,** 180–8 (2012).
50. Yoshida, R. *et al.* The regulatory domain of SRK2E/OST1/SnRK2.6 interacts with ABI1 and integrates abscisic acid (ABA) and osmotic stress signals controlling stomatal closure in Arabidopsis. *J. Biol. Chem.* **281,** 5310–5318 (2006).
51. Boudsocq, M., Droillard, M. J., Barbier-Brygoo, H. & Laurière, C. Different phosphorylation mechanisms are involved in the activation of sucrose non-fermenting 1 related protein kinases 2 by osmotic stresses and abscisic acid. *Plant Mol. Biol.* **63,** 491–503 (2007).
52. Fujii, H. & Zhu, J.-K. Osmotic stress signaling via protein kinases. *Cell. Mol. Life Sci.* **69,** 3165–73 (2012).
53. Yoshida, T., Mogami, J. & Yamaguchi-Shinozaki, K. ABA-dependent and ABA-independent signaling in response to osmotic stress in plants. *Curr. Opin. Plant Biol.* **21C,** 133–139 (2014).
54. Hu, Y. & Yu, D. BRASSINOSTEROID INSENSITIVE2 Interacts with ABSCISIC ACID INSENSITIVE5 to Mediate the Antagonism of Brassinosteroids to Abscisic Acid during Seed Germination in Arabidopsis. *Plant Cell* **1,** 1–16 (2014).
55. Cai, Z. *et al.* GSK3-like kinases positively modulate abscisic acid signaling through phosphorylating subgroup III SnRK2s in Arabidopsis. *Proc. Natl. Acad. Sci. U. S. A.* **111,** 9651–6 (2014).
56. Zheng, Z. *et al.* The protein kinase SnRK2.6 mediates the regulation of sucrose metabolism and plant growth in Arabidopsis. *Plant Physiol.* **153,** 99–113 (2010).
57. Vilela, B., Nájar, E., Lumbreras, V. & Leung, J. Casein Kinase 2 negatively regulates abscisic acid-activated SnRK2s in the core abscisic acid-signaling module. *Mol. Plant* **2,** 1–13 (2015).
58. Lozano-Juste, J. & León, J. Nitric oxide modulates sensitivity to ABA. *Plant Signal. Behav.* **5,** 314–316 (2010).
59. Neill, S. *et al.* Nitric oxide, stomatal closure, and abiotic stress. *J. Exp. Bot.* **59,** 165–76 (2008).

60. Wang, P. *et al.* Nitric oxide negatively regulates abscisic acid signaling in guard cells by S-nitrosylation of OST1. *Proc. Natl. Acad. Sci.* **112,** 613–618 (2015).
61. Meinhard, M. & Grill, E. Hydrogen peroxide is a regulator of ABI1, a protein phosphatase 2C from Arabidopsis. *FEBS Lett.* **508,** 443–446 (2001).
62. Meinhard, M., Rodriguez, P. L. & Grill, E. The sensitivity of ABI2 to hydrogen peroxide links the abscisic acid-response regulator to redox signalling. *Planta* **214,** 775–782 (2002).

Table 1. Primers used in PCR for genotype and transcript analyses.

Gene	Forward Primer	Revers Primer
ABI1	GAATGGAGCTCGTGTTTTCGG	GTTCAAGGGTTTGCTCTTGAGT
18S rRNA	CGGCTACCACATCCAAGGAA	GCTGGAATTACCGCGGCT
RBCS1-B	ATGGCTTCCTCTATGCTCTCCT	TTAAGCATCAGTGAAGCTTGGG
CHS	CTTGACTCCCTCGTCGGTCA	CAAGACGACTGTCTCAACAGTG
PAP1	GCTCTGATGAAGTCGATCTTCT	CTACCTCTTGGCTTTCCTCTA
G17	GTACGTATTTTTACAACAATTACCAAC	
GFP		TCTTGAAGAAGTCGTGCCGCTT

Table 2. Primers used in quantitative RT-PCR analysis.

Gene	Forward Primer	Reverse Primer
18S rRNA	CGGCTACCACATCCAAGGAA	GCTGGAATTACCGCGGCT
CHS	AAGCGCATGTGCGACAAG	TCCTCCGTCAGATGCATGTG
Gln1;4	GATCTTTGAAGACCCTAGTGTTG	TTGGTTTAGGGTCTAGAGACAGA
NCED3	GCCGAAGATTCATCGAACAT	CGAGTTGATTCACCGGTTTT
RD29b	AAAAGAGAGGCACCGACTCA	CCGTTGACCACCGAGATAGT
RAB18	CGGATGTTTGTTTCTGGAGTG	CGGGGTTTTGTTTGAAGATG
LEA3-4	ACAAGACGGGTGGATTCTTGA	TGCATCAGCTGCACCCATT
TSPO	ACGCTCTTCGCTACGTATTTCC	ACGACGAGGACTTAGCTCGATT
AREB1	GCTTTGTCCAAGGTGCTTCTG	CAGGCGACACAGCACCAA
ABF3	GAATTCCGCAGAGGCAACA	CCAGCCCTGACCAAAAACTC
DIN6	TCCATCACTGCACGTCACTT	ATATTCCGCCACCTCTTTCC
SEN5	GCGAAACTCTCTCCGACTTC	CCACAGAACAACCTTTGACG

Table 3. Regulation of ABA signaling directly by multiple cellular signaling pathways.

Regulator	Target	Effect	Reference
H_2O_2	AtHAB1	Inhibits the interaction of HAB1 and SnRK2s	47,61,62
AtROP11	AtABI1	Protect ABI1 phosphatase activity	48,49
AtBIN2, AtBIL1, AtBIL2	AtSnRK2.2, AtSnRK2.3,	Phosphorylates and activates SnRK2.2 and SnRK2.3	55
	ABI5	Phosphorylates and stabilizes ABI5	54
ZmCK2	ZmSnRK2.6/OST1	Enhances the interaction between SnRK2.6/OST1 and ABI1 and degrades SnRK2.6/OST1	57
NO	AtSnRK2.6/OST1	S-nitrosylation and repression of SnRK2.6	60

At: *Arabidopsis thaliana*; Zm: *Zea maize*

Figure 1

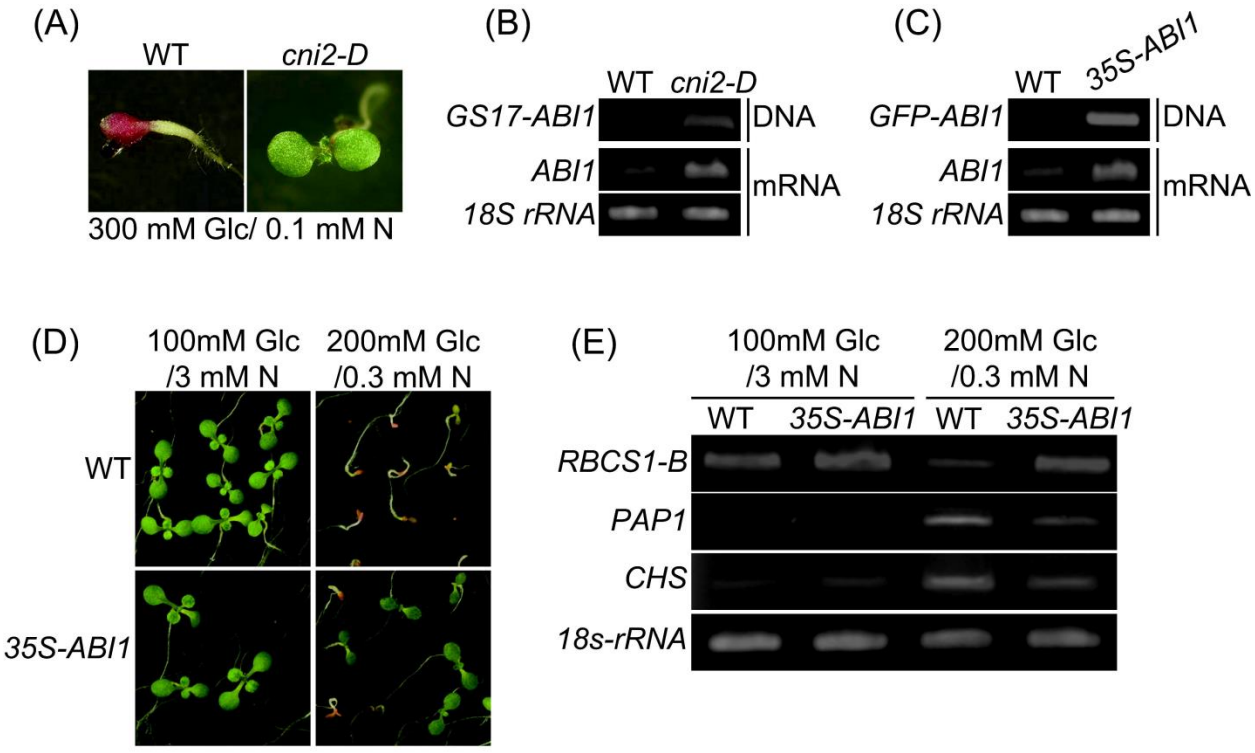
(A)
WT
cni2-D
300 mM Glc/ 0.1 mM N
(B)
WT
cni2-D
GS17-ABI1
DNA
ABI1
mRNA
18S rRNA
(C)
WT
35S-ABI1
GFP-ABI1
DNA
ABI1
mRNA
18S rRNA
(D)
100mM Glc /3 mM N
200mM Glc /0.3 mM N
WT
35S-ABI1
(E)
100mM Glc /3 mM N
200mM Glc /0.3 mM N
WT
35S-ABI1
WT
35S-ABI1
RBCS1-B
PAP1
CHS
18s-rRNA

Figure 1. Isolation of *cni2-D* transgenic plant and C/N responses of *35S-ABI1*.

(A) Screening of Arabidopsis FOX hunting population with medium containing 300 mM glucose (Glc) and 0.1 mM nitrogen (N). (B) Genomic PCR using primers for the *pBIG* vector (GS17) and *ABI1* (top panel) and RT-PCR of *ABI1* mRNA transcripts (middle panel) in WT and *cni2-D* plants. *18S rRNA* was used as an internal control (bottom panel). (C) Genomic PCR using primers for inserted GFP and *ABI1* (top panel) and RT-PCR of *ABI1* mRNA transcripts (middle panel) in WT and *35S-ABI1* plants. *18S rRNA* was used as an internal control (bottom panel). (D) Post-germinative growth phenotypes of WT and *35S-ABI1* transgenic plants grown under normal (100 mM Glc/3 mM N) and high C/low N stress (200 mM Glc/0.3 mM N) conditions. Images were taken 7 days after germination. (E) RT-PCR analysis of *RBCS1-B, CHS* and *PAP1* mRNA transcripts in WT and *35S-ABI1* plants grown under the same conditions as in Fig. 1D. *18S rRNA* was used as an internal control. WT, wild-type (Col-0).

Figure 2

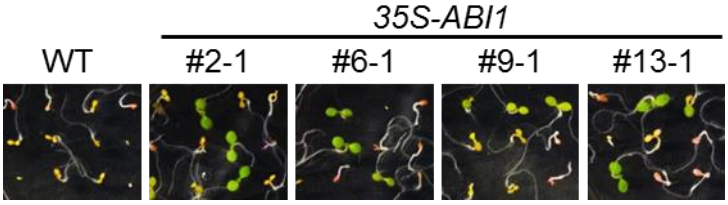

Figure 2. C/N response phenotype of *ABI1* over-expressors..

Post-germinative growth of WT and four-independent lines of 35S-ABI1 plants grown on high C/low N stress medium (200 mM Glc/0.3 mM N). Images were taken at 7 days after germination. WT, wild-type (Col-0).

Figure 3

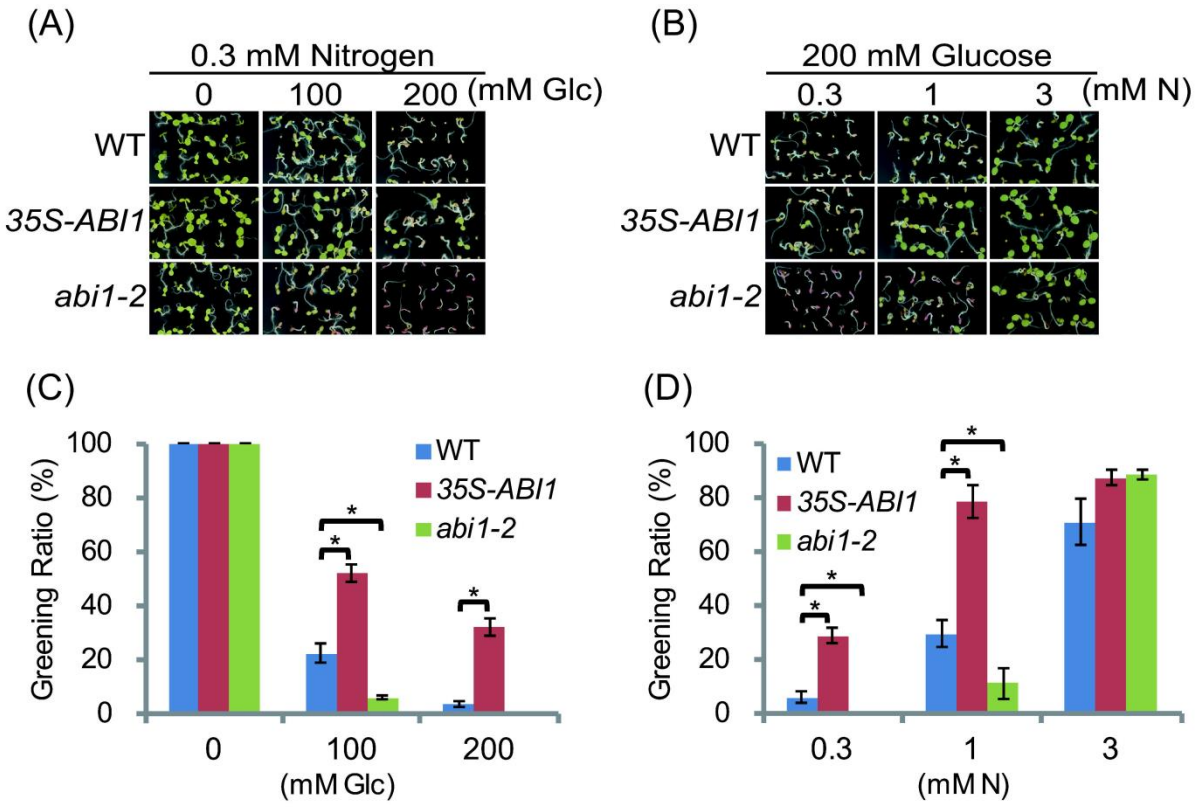
(A)
0.3 mM Nitrogen
0
100
200 (mM Glc)
WT
35S-ABI1
abi1-2
(B)
200 mM Glucose
0.3
1
3 (mM N)
WT
35S-ABI1
abi1-2
(C)
Greening Ratio (%)
100
80
60
40
20
0
WT
35S-ABI1
abi1-2
0
100
200
(mM Glc)
(D)
Greening Ratio (%)
100
80
60
40
20
0
WT
35S-ABI1
abi1-2
0.3
1
3
(mM N)

Figure 3. Post-germinative growth of *35S-ABI1* and *abi1-2* plants under different C/N conditions.

(A) Post-germinative growth phenotype of WT, *35S-ABI1* and *abi1-2* plants germinated on media containing 0.3 mM N with 0, 100 and 200 mM Glc. Images were taken 7 days after germination. (B) Post-germinative growth phenotype of WT, *35S-ABI1* and *abi1-2* plants germinated on medium containing 200 mM Glc with 0.3, 1 and 3 mM N. Images were taken 7 days after germination. (C) Greening ratios of WT, *35S-ABI1* and *abi1-2* seedlings; growth conditions are described in Fig. 2A. Each treatment involved 20-40 seedlings. Means ± SD of three independent experiments are shown. (D) Greening ratios of *35S-ABI1* and *abi1-2* seedlings grown under the conditions shown in Fig 2B. Each treatment involved 20-40 seedlings. Means ± SD of three independent experiments are shown. WT, wild-type (Col-0). Asterisk indicates significant differences determined by Dunnet analysis ($p<0.05$).

Figure 4

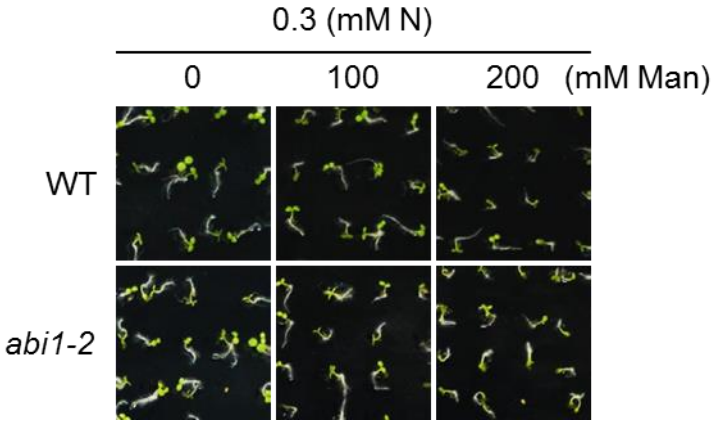

Figure 4. Osmotic stress response of *abi1-2* mutants.

Post-germinative growth phenotypes of WT and *abi1-2* mutants grown on medium containing 200 mM mannitol (Man)/0.3 mM N. Images were taken at 7 days after germination. WT, wild-type (Col-0).

Figure 5

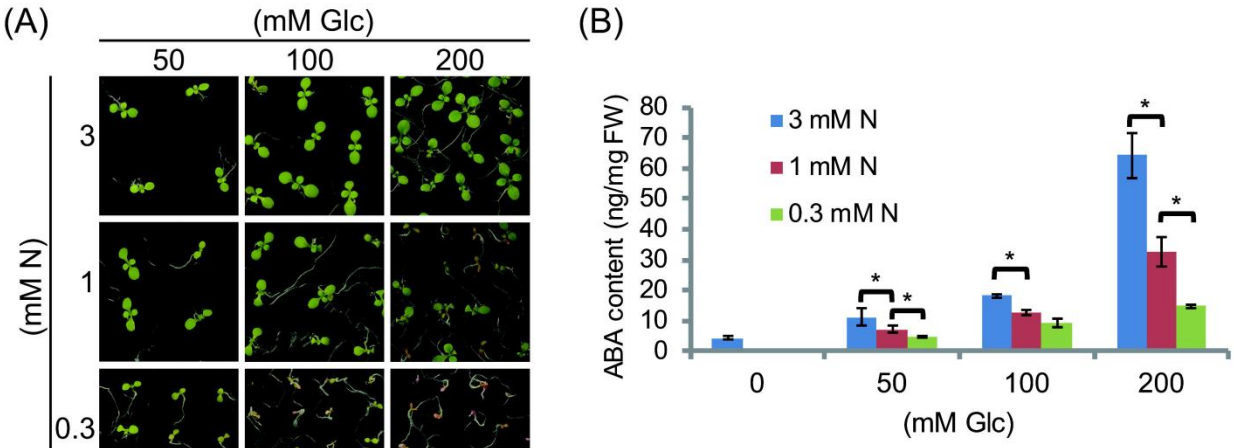
(A)
(mM Glc)
50
100
200
(mM N)
3
1
0.3
(B)
ABA content (ng/mg FW)
80
70
60
50
40
30
20
10
0
3 mM N
1 mM N
0.3 mM N
*
0
50
100
200
(mM Glc)

Figure 5. ABA content in response to C/N status.

(A) Post-germinative growth phenotype of WT plants grown in C/N medium containing combinations of 50, 100 and 200 mM Glc and 3, 1 and 0.3 mM N. (B) Endogenous level of ABA of WT plants grown under the C/N conditions indicated in Fig. 3A and 0 mM Glc/3 mM N. Seedlings were harvested 7 days after germination. Means ± SD of four independent experiments are shown. WT, wild-type (Col-0). Asterisk indicates significant differences in response to limited N condition determined by Tukey analysis (p<0.05).

Figure 6

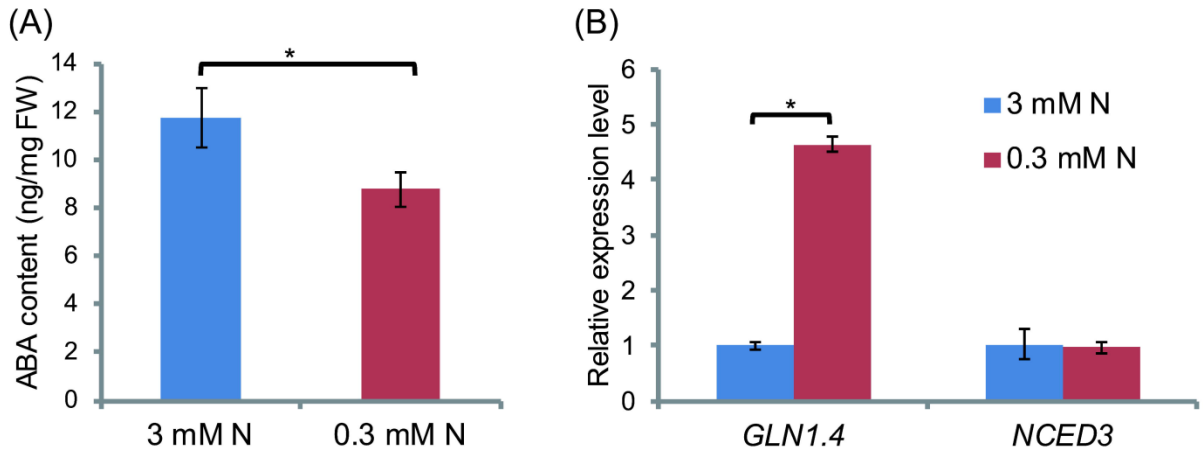
(A)
ABA content (ng/mg FW)
14
12
10
8
6
4
2
0
*
3 mM N
0.3 mM N
(B)
Relative expression level
6
5
4
3
2
1
0
*
3 mM N
0.3 mM N
GLN1.4
NCED3

Figure 6. ABA amounts and *NCED3* expression in response to transiently limited N treatment.

WT plants grown on control medium (100 mM Glc/3 mM N) for 7 days after germination were transferred to control N (3 mM N) or limited N (0.3 mM N) medium. Plants were harvested 3 days after transfer. (A) ABA quantification and (B) qRT-PCR analysis. Error bars represent SE (n=4). The level of expression of each gene was normalized relative to that of *18S rRNA* in the same sample and relative expression levels were compared with those of WT plants transferred to control N condition. Means ± SD of four independent experiments are shown. WT, wild-type (Col-0). Asterisk indicates significant differences in response to limited N condition determined by Student's *t* test ($p<0.05$).

Figure 7

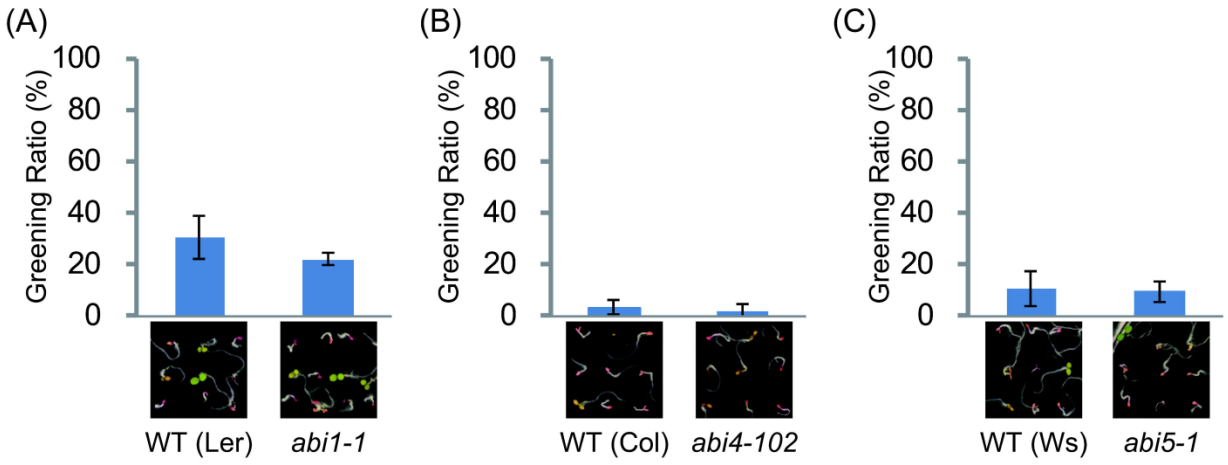
(A)
Greening Ratio (%)
100
80
60
40
20
0
WT (Ler)
abi1-1
(B)
Greening Ratio (%)
100
80
60
40
20
0
WT (Col)
abi4-102
(C)
Greening Ratio (%)
100
80
60
40
20
0
WT (Ws)
abi5-1

Figure 7. Post-germinative growth of ABA insensitive mutants under C/N stress condition.

Greening ratio and post-germinative growth phenotype of the ABA insensitive mutants (A) *abi1-1* (B) *abi4-102* and (C) *abi5-1* grown in high C/low N (200 mM Glc/ 0.3 mM N) condition. WT plants for each mutant were Ler for *abi1-1*, Col-0 for *abi4-102* and Ws-2 for *abi5-1*. Each treatment involved 20-40 seedlings. Means ± SD of three independent experiments are shown. Images were taken 7 days after germination.

Figure 8

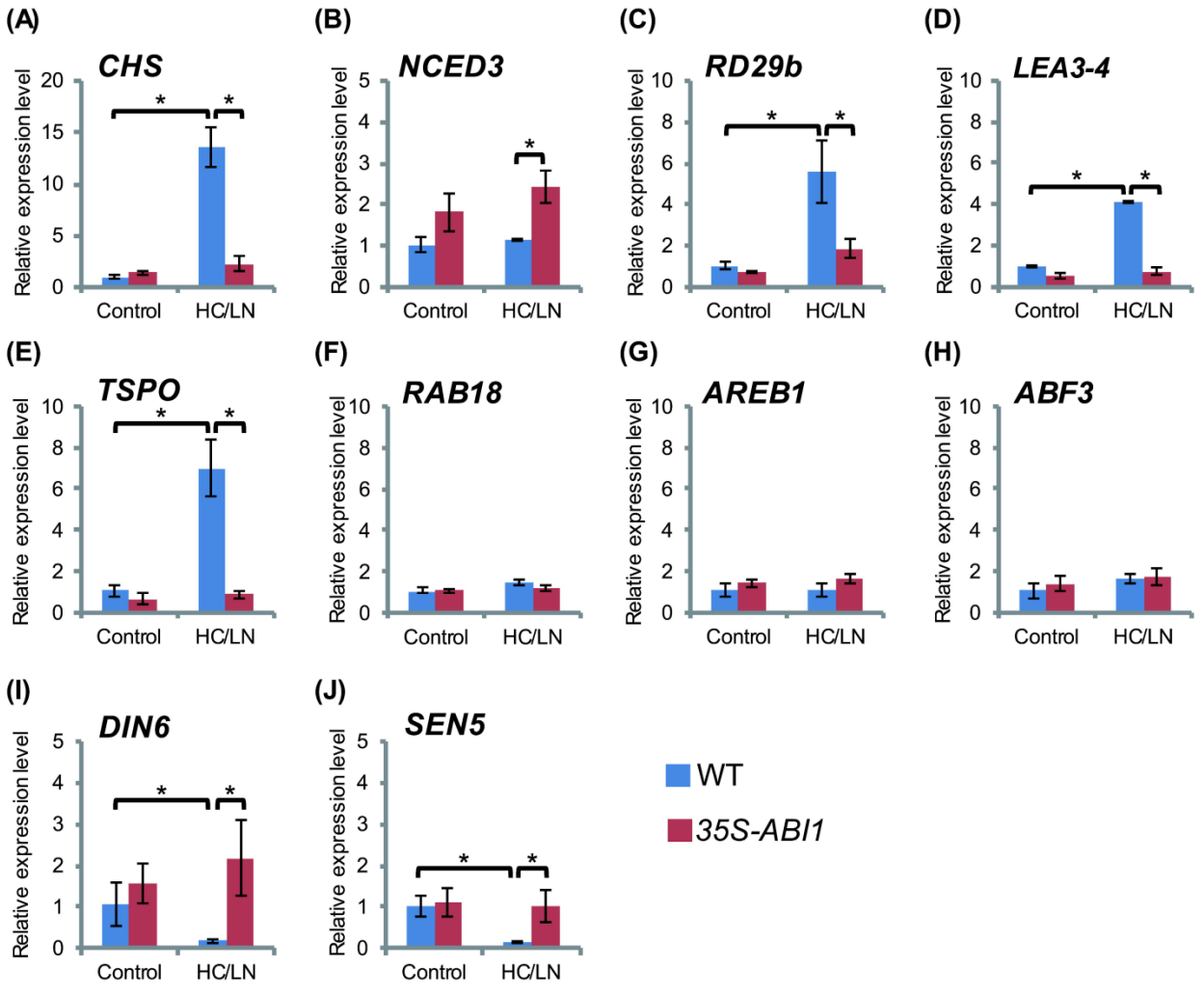
(A)
CHS
Relative expression level
20
15
10
5
0
Control
HC/LN
(B)
NCED3
5
4
3
2
1
0
(C)
RD29b
10
8
6
4
2
0
(D)
LEA3-4
(E)
TSPO
(F)
RAB18
(G)
AREB1
(H)
ABF3
(I)
DIN6
(J)
SEN5
WT
35S-ABI1

Figure 8. Transcripts levels of C/N- and ABA-related marker genes.

WT and *35S-ABI1* plants were grown in normal (100 mM Glc/3 mM N; Control) or high C/low N (200 mM Glc/0.3 mM N; HC/LN) for 7 days after germination, and expression levels were analyzed by qRT–PCR. The level of expression of each gene was normalized relative to that of *18S rRNA* in the same sample, and relative expression levels were compared with those of WT in normal C/N condition. Means ± SD of three independent experiments are shown. WT, wild-type (Col-0). Asterisk indicates significant differences determined by Tukey analysis ($p<0.05$).

CHAPTER II

Characterization of ubiquitin ligase SlATL31 and proteomic analysis of 14-3-3 targets in tomato fruit tissue (*Solanum lycopersicum* L.)

Summary

The 14-3-3 proteins participate in many aspects of plant physiology by interacting with phosphorylated proteins and thereby regulating target protein functions. In Arabidopsis plant, the ubiquitin ligase ATL31 controls 14-3-3 stability via both direct interaction and ubiquitination, and this consequently regulates post-germinative growth in response to carbon and nitrogen nutrient availability. Since 14-3-3 proteins regulate the activities of many key enzymes related to nutrient metabolism, one would anticipate that they should play an essential role not only in vegetative but also in reproductive tissue. Because fruit yield largely depends on carbon and nitrogen availability and their utilization, the function of 14-3-3 proteins was analyzed in tomato fruit tissue. Here, I isolated and characterized an ubiquitin ligase SlATL31 (Solyc03g112340) from tomato and demonstrated that SlATL31 has ubiquitin ligase activity as well as interaction with tomato 14-3-3 proteins, suggesting the possibility that the SlATL31 functions as an ubiquitin ligase for 14-3-3 similarly to its Arabidopsis ortholog. Furthermore, I performed proteomic analysis of 14-3-3 interacting proteins and identified 106 proteins as putative 14-3-3 targets including key enzymes for carbon metabolism and photosynthesis. This 14-3-3 interactome result and available transcriptome profile suggest a considerable yet complex role of 14-3-3 proteins in tomato fruit tissue.

Introduction

The 14-3-3 proteins are highly conserved versatile regulator in eukaryotic organism. 14-3-3 dimers generally interact with phosphorylated target proteins and regulate target functions by modifying their features, including subcellular localization, enzymatic activity, stability and protein-protein interaction[1,2,3]. In plants, 14-3-3 target proteins participate in a wide range of physiological pathways, including primary metabolism,

hormone signaling, cell growth and division, and response to multiple environmental stresses[3,4,5]. To date, proteomic analyses have identified over 300 14-3-3 target proteins in land plants[6,7], reflecting the complexity of the network of 14-3-3 regulation in plant physiology.

Our laboratory previously reported that 14-3-3 proteins are essential regulators involved in plant adaptation to the balance between carbon and nitrogen (C/N)[8]. The availability of C/N is one of the most crucial factors in regulating plant metabolism and development[9,10,11]. Mutant screening analysis using Arabidopsis enabled the isolation of the ubiquitin ligase ATL31 as a novel C/N regulatory protein[12]. ATL31 is a member of the plant-specific ubiquitin ligase ATL family, consisting of proteins containing transmembrane-like hydrophobic regions at the N-terminus, a conserved GLD motif, a RING-H2 type zinc finger domain (RING domain) and a non-conserved C-terminal region[13]. Subsequent proteomic and genetic analyses demonstrated that ATL31 regulates the stability of 14-3-3 proteins by direct ubiquitination, resulting the regulation of post-germinative growth in response to C/N-nutrient status[8,14]. Enzymes involved in primary metabolism, including glutamine synthase, H^+-ATPase, sucrose phosphate synthase, sucrose synthase, starch synthase and nitrate reductase, have been identified as 14-3-3 targets in Arabidopsis plants[35,15].

The tomato (*Solanum lycopersicum* L.) is a major crop plant and model system for fleshy fruit development[16,17]. The genome sequence of this species was published in 2012[18]. As crop productivity and fruit quality are affected by the availability of carbon and nitrogen[19], I speculated that 14-3-3 proteins likely serve as metabolic regulators in tomato, controlling tomato fruit development and quality. In tomato, 14-3-3 proteins function in immune responses[20,21], nutrient responses[22] and other stress responses[23]. Conversely, their function during fruit development remains poorly understood. This interactome analysis provided the first report of the overview of 14-3-3 targets in tomato fruit. My results are discussed in the context of the function of 14-3-3 proteins in sucrose and other carbon metabolism including photosynthesis in tomato fruit, as well as more generally with regard to reprogramming of metabolism following alterations in the protein degradative machinery.

Materials and methods

Plant material and growth condition

The tomato (*Solanum lycopersicum* L.) cultivar Micro-Tom[24] was grown in 9 cm pots containing Jiffy-Mix soil with approximately 4 mM nitrogen (Jiffy, Japan), supplemented with HYPONeX nutrition mixture (6% nitrogen, 10% phosphorous; HYPONeX, Japan, http://www.hyponex.co.jp), at 25°C and 16:8 hour light:dark cycles.

Plasmid construction

The coding sequences of truncated *SlATL31* (SlATL31Thr84-Val398), full length *TFT3* and *TFT10* were amplified from a tomato cDNA library. Truncated *SlATL31* harboring a point mutation conferring a Cys138Ser substitution (C138S) within the RING domain was produced by site directed mutagenesis. Primers used for amplification and point mutagenesis are listed in Table 4. The fragments were cloned into pENTR/D-TOPO vector and subsequently transferred into destination vectors following the Gateway instruction manual (Invitrogen, USA). The identities of all PCR products and inserts were confirmed by DNA sequencing. The truncated *SlATL31* and *SlATL31C138S* fragments was transferred from pENTR/D-TOPO into the pDEST-mal vector[25] following the Gateway instruction manual (Invitrogen, USA), generating bacterial plasmids expressing the recombinant SlATL31 and SlATL31C138S proteins fused with maltose binding protein (MBP) (MBP-SlATL31 and MBP-SlATL31C138S).

Generation and screening of transgenic tomato lines

The full length *14-3-3λ* cDNA inserted pENTR/D-TOPO plasmid[14], was recombined into the pGWB12 T-DNA binary vector[26] according to the Gateway instruction manual (Invitrogen, USA), thus placing the full-length *14-3-3λ* gene under control of the 35S promoter (*FLAG-14-3-3λ*). *Agrobacterium (Rhizobium) tumefaciens* GV2260 using the electroporation method. The constructs were transformed into wild-type 'Micro-Tom' according to a procedure described by[27]. The transgenic calli were screened on Murashige and Skoog (MS) agar plates containing kanamycin (100 mg /L)[28]. Only

diploid plants harboring single copy of the transgene were selected from the regenerated plants as the T_0 generation.

In vitro ubiquitination assay

The pDEST-mal plasmids expressing MBP-SlATL31 and MBP-SlATL31C138S fusion proteins were independently introduced into *E.coli* strain BL21 (DE3) pLysS (Novagen, Germany). The resulting recombinant proteins were purified by amylose affinity chromatography, according to the manufacturer's instructions (New England BioLabs, USA). Ubiquitination assays were performed as described[12], with minor modifications. Briefly, 500 ng of MBP-SlATL31 or MBP-SlATL31C138S were incubated in 30 µL of reaction buffer (40 mM Tris-HCl, pH 7.5, 5 mM $MgCl_2$, 2 mM ATP, 2 mM dithiothreitol) containing 50 ng of mouse E1 (Wako, Japan), 250 ng of UbcH5a (Wako, Japan) of E2 and 9 µg of ubiquitin (Sigma-Aldrich, USA), for 0 to 60 min at 30°C. The reactions were terminated by addition of SDS sample buffer [62.5 mM Tris-HCl, pH 6.8, 10% glycerol (v/v), 2% SDS (w/v), 5% β-mercaptoethanol (v/v) and 0.01% bromophenol blue (w/v)]. The reaction products were analyzed by SDS-PAGE followed by western blotting using anti-ubiquitin antibody (FK2; Nippon Bio-Test Laboratories Inc., Japan) and anti-MBP antibody (New England BioLabs, USA).

Yeast two-hybrid assay

Yeast strain EGY48/pJK103 was used for the two-hybrid assays. The truncated *SlATL31* with encoding the Cys138Ser substitution was subcloned into pEG202gw destination vector as bait, and the full-length sequence of *TFT3* and *TFT10* were subcloned into pJG4-5gw destination vector as prey (pEG202gw and pJG4-5gw vectors were kindly provided by Dr. Hironori Kaminaka, Tottori University, Japan). pJG4-5gw vectors containing full length *14-3-3χ* or *14-3-3λ* previously described[14]. Vectors pEG202 and pJG4-5 were used as empty vector controls. Yeast transformation was performed using the Frozen-EZ yeast Transformation II Kits (Zymo Research, USA), according to the manufacturer's instructions. Handling of yeast cultures and *β*-galactosidase assay were performed as described in the Yeast Protocols Handbook (Clontech, Japan).

Immunoprecipitation of 14-3-3 complex along with FLAG tagged 14-3-3 protein from tomato fruit tissue

Expanding green tomato fruit was harvested from wild-type (WT) and *FLAG-14-3-3λ* transgenic strains, immediately frozen in liquid nitrogen and stored at -80°C before use. Samples were ground in liquid nitrogen and lysed with extraction buffer [100 mM Tris-HCl, pH7.5, 10% glycerol (v/v), 150 mM NaCl, 5 mM $MgCl_2$, 1 mM EDTA, 0.5% Triton X-100 (v/v)] supplemented with 10 μM MG132, complete protease inhibitor mixture (Roche Applied Science, Germany) and PhosSTOP phosphatase Inhibitor cocktail tablets (Roche Applied Science, Germany). After the removal of insoluble materials by centrifugation twice at 20,000×*g* for 5 min at 4°C, protein concentrations were determined by Bradford method (Bio-Rad, USA) and normalized. Anti-FLAG M2 antibody conjugated to magnet beads (Sigma-Aldrich, USA) was added to the extracts, which were gently shaken for 1 h at 4°C on a rotary shaker. The beads were washed three times with extraction buffer and bound proteins were eluted with FLAG peptides (3 μg /μL) (Sigma-Aldrich, USA). The eluted proteins were dissolved in SDS sample buffer prior to SDS-PAGE, followed by western blotting using anti-FLAG M2 antibody (Sigma-Aldrich, USA) or MS analysis.

Peptide preparation for LC-MS/MS analysis

Immunoprecipitated proteins were separated on a ready-made 10% polyacrylamide (w/v) gel (Perfect NT Gel; DRC, Japan) and stained with SYPRO Ruby (Lonza, Switzerland) as described in the manufacture's instructions. The excised gels were dehydrated with 100% acetonitrile and then incubated in 10 mM dithiothreitol/50 mM ammonium bicarbonate for 45 min at 56°C with shaking. After reduction, the gels were incubated in 55 mM iodoacetamide/50 mM ammonium bicarbonate for 30 min at room temperature in dark with shaking. After alkylation, the gels washed with 25 mM ammonium bicarbonate and dehydrated with 100% acetonitrile. The dried gels were incubated in 50 mM ammonium bicarbonate containing sequence grade modified trypsin (Promega, USA) for 16 h at 37°C. The digested peptides were eluted by 50% acetonitrile (v/v) /5% formic acid (v/v) from the gels and dried using an evaporator. The peptides were dissolved in 5% acetonitrile (v/v) /0.1% formic acid (v/v) and filtered by

the Ultrafree-MC Centrifugal Filtrers (PVDF 0.45 μm; Millipore, USA) to avoid contamination of gel pieces.

MS analysis and protein identification

Peptide identification was performed using an EASY-nLC 1000 liquid chromatograph coupled to an Orbitrap Elite Mass Spectrometer (Thermo Scientific, USA). Trypsin-digested peptides were separated on a nano-capillary column (NTCC-360/75-3-125; Nikkyo Technos, Japan). The mobile phase consisted of 0.1% formic acid (v/v) in water (buffer A) and 0.1% formic acid (v/v) in acetonitrile (buffer B). The peptides were eluted at a flow of 300 nL/min, using a three-step linear gradient: from 0 to 35% B for 55 min, from 35 to 100% B for 5 min and 100% B for 8 min. Survey full-scan mass spectra were acquired in the Orbitrap analyzer. The scanned mass range was 300 to 1,500 *m/z*, at a resolution of 120,000 at *m/z* 400, and the ten most intense ions were sequentially isolated, fragmented (collision-induced dissociation at 35 eV) and measured in the linear ion trap. Protein identification was performed by SEQUEST algorithm embedded in Proteome Discoverer 1.4 software (Thermo Scientific, USA) against TAIR10 (http://www.arabidopsis.org/index.jsp) and ITAG2.4 (http://solgenomics.net/) with the following parameters: a precursor ion tolerance of 10 ppm, a product ion mass tolerance of 0.8 Da, trypsin as the enzyme allowing up to two missed cleavage, carbamidomethylation on cysteine as a fixed modification and oxidation of methionine as a variable modification. To guarantee the accuracy of the result, an automatic decoy database search strategy was employed to estimate false discovery rate (FDR), with only FDR values less than 1% were considered as significant. The matched peptides were accepted when the Xcorr values for singly (z = 1), doubly (z = 2) and triply (z = 3) charged ions were ≥1.5, ≥2.0 and ≥2.5, respectively. To identify putative 14-3-3-specific interactions, proteins detected in at least two of three replicates with SEQUEST ion score >10 were selected and the results of *FLAG-14-3-3λ* plants compared with negative control WT plants.

Prediction of 14-3-3 binding sites

All protein sequences were obtained from the tomato database (ITAG2.4, https://solgenomics.net/).The FASTA format file was uploaded to the 14-3-3-Pred website (http://www.compbio.dundee.ac.uk/1433pred/). The 14-3-3 binding sites of each protein were identified based on the cut-off criteria, i.e. ANN ≥0.55, PSSM ≥0.80, SVM ≥0.25 and Consensus ≥0.50[29].

Results and discussion

Isolation of an ubiquitin ligase SlATL31 from tomato

The entire sequence of the tomato genome was searched for genes encoding orthologous protein to Arabidopsis ATL31. BLAST analysis of the Sol genomic database (https://solgenomics.net/) returned several proteins exhibiting high homology of amino acid sequences to Arabidopsis ATL31. I found that *Solyc03g112340* encodes the protein most closely related to Arabidopsis ATL31 (Fig. 9). The Cys and His residues, which are essential to form the zinc finger structure of RING domain, showed conservation in Solyc03g112340 protein (Fig. 10), and the hydropathy plot of the Solyc03g112340 protein showed the presence of two hydrophobic regions at the N-terminus (Fig. 11), suggesting that this protein functions as a membrane-localized ubiquitin ligase. In addition, the C-terminal region of Solyc03g112340 protein contained putative 14-3-3 binding motifs, which had been shown to mediate direct interactions between ATL31 and 14-3-3 proteins in Arabidopsis[14] (Fig. 10). Taken together, these facts implicate Solyc03g112340 as the functional homologue of ATL31 protein in tomato plants. Microarray data of The Tomato Genome Consortium (2012)[18] indicated that *Solyc03g11234* gene expression is upregulated during fruit ripening (Fig. 12), suggesting that *Solyc03g11234* is involved in tomato fruit development. Thus, the *Solyc03g112340* gene was therefore named *SlATL31* and the biochemical function of SlATL31 protein was further examined.

SlATL31 has ubiquitin ligase activity

The ubiquitin ligase activity of SlATL31 was examined by *in vitro* ubiquitination assays. As the N-terminal hydrophobic region of ATL family proteins have been

reported to inhibit sufficient expression of the recombinant fusion proteins in *E. coli*[12,30], this region (residues Met1-Arg83) of SlATL31 was deleted, and the remaining region (Thr84-Val398) was used to generate an MBP-SlATL31 fusion protein. Following the ubiquitination reaction of the purified MBP-SlATL31 protein, the formation of a heterogeneous collection of higher molecular mass proteins were detected by western blotting using anti-ubiquitin and anti-MBP antibodies (Fig. 13), indicating that MBP-SlATL31 has ubiquitin ligase activity. In addition, replacement of the conserved Cys138 in the RING domain of SlATL31 with serine (SlATL31C138S) resulted in a loss of the ubiquitination activity of MBP-SlATL31C138S, further confirming that SlATL31 functions as a RING-type ubiquitin ligase.

SlATL31 interacts with tomato 14-3-3 proteins

Among the 13 members of the Arabidopsis 14-3-3 family proteins, two isoforms, 14-3-3χ and 14-3-3λ, had been demonstrated to possess the highest affinity toward AtATL31[14]. To date, 12 gene members of the 14-3-3 family, named *TFTs*, have been identified in the tomato genome[23]. Based on the phylogenetic analyses[31], TFT3 and TFT10 were selected as the homologues of 14-3-3χ and 14-3-3λ, respectively. The physical interactions between these two proteins and SlATL31 were analyzed by yeast two-hybrid (Y2H) assays. As the N-terminal hydrophobic region (Met1-Arg83) of SlATL31 inhibited its expression and nuclear localization in yeast, this region was removed. In addition, the RING-mutated *SlATL31C138S* construct was applied to the analysis, because RING-active ATL31 promotes the degradation of 14-3-3 proteins, thus disturbs the interaction analysis[8]. These Y2H assays confirmed that SlATL31C138S protein interacted with both TFT3 and TFT10 proteins (Fig. 14). Moreover, the SlATL31 protein also interacted with both 14-3-3χ and 14-3-3λ proteins (Fig. 14). Our laboratory previously demonstrated that Arabidopsis ATL31 with mutation in the third 14-3-3 binding motif could bind to 14-3-3 protein through the three other binding motifs while the third motif could also mediate this interaction[14]. Thus, the three putative 14-3-3 binding motifs conserved in SlATL31 were likely sufficient for the interaction with 14-3-3 proteins (Fig. 8B). When taken together, these data support the hypothesis that the SlATL31 interacts with 14-3-3 protein at the conserved 14-3-3

binding motifs at the C-terminal region[8,14] and that the biochemical function of the ubiquitin ligase ATL31 to modulate the 14-3-3 stability might conserved between Arabidopsis and tomato plants.

Recently, Tang et al[32] reported that CUL4-DDB1-DET1 ubiquitin ligase complex regulates the proteasomal degradation of a GOLDEN 2-LIKE (GLK2) transcription factor which regulates chlorophyll accumulation and plastid development in tomato fruit, clearly indicating ubiquitin-proteasome system plays a critical role in fruit development[33]. Further investigation of biochemical and physiological function of SlATL31 ubiquitin ligase will further reveal the impact of ubiquitin modification system for the regulation of fruit development and primary metabolism in tomato.

Immunoprecipitation and MS analysis of 14-3-3 targets in tomato fruit tissue

In Arabidopsis plants, 14-3-3 proteins have been reported to regulate the activities of enzymes involved in primary metabolism as well as protein stability of transcription factors regulating organ development via direct physical interactions[34]. However, 14-3-3 functions in fruit tissue remain unclear. To uncover the function of 14-3-3 proteins in fruit, I established transgenic tomato plants constitutively expressing FLAG tagged 14-3-3λ (*FLAG-14-3-3λ*) and performed a 14-3-3 interactome analysis (see Materials and methods for details). Expanding green fruits of this transgenic tomato plant, which have a normal visible phenotype similar to that of the wild-type tomato, were harvested and utilized in affinity purification of 14-3-3 complexes. Western blotting with anti-FLAG antibody (Fig. 15) and MS/MS analysis using Arabidopsis database (TAIR10) (Table 5) resulted in the specific identification of 14-3-3λ protein in all specimens from FLAG-14-3-3λ expressing transgenic plants, but not in specimens from wild-type plants. In addition to 14-3-3λ protein, several endogenous tomato TFT proteins, including TFT2, 3, 5, 6, 7, 8 and 11, were detected by MS/MS analysis using tomato database (ITAG2.4). As 14-3-3 proteins form both homo- and hetero-dimers in order to catch the target proteins, these results suggested that this procedure resulted in the successful purification of active 14-3-3 complexes from tomato fruit (Table 6). Although TFT10 was not identified in this MS/MS analysis, the expression level of *TFT10* gene was

significantly increased during the ripening stage, thus I cannot exclude the possibility that TFT10 also functions in tomato fruit development[18] (Fig. 16).

Using several criteria (see Materials and methods for details), a total of 106 proteins were identified as putative 14-3-3 target proteins in tomato fruit. These included key proteins related to carbon metabolism, protein biosynthesis, signal transduction, cytoskeleton, vesicle traffic and ion transportation (Table 7). It is well characterized that 14-3-3 proteins recognize at least three types of binding motifs in the target proteins, K/RxxS$_p$/T$_p$xP, K/RxxxS$_p$/T$_p$xP and YT$_p$V, where x represents any amino acid residue and "S$_p$/T$_p$" represents phosphorylated serine or threonine[35]. Then the 14-3-3 binding site of all the 106 resulted 14-3-3 binding proteins in tomato fruit was predicted using advanced 14-3-3 binding phosphosite prediction database, 14-3-3-Pred (http://www.compbio.dundee.ac.uk/1433pred/)[29]. The results indicated 75 proteins of the interactors contained predicted 14-3-3 binding motifs with high confidence levels (Table 7).

The following discussion focuses on the putative 14-3-3 target proteins involved in carbohydrate metabolism and photosynthesis.

Carbohydrate metabolism: Sucrose metabolism

In this study, I identified several enzymes involved in sucrose metabolism were found to interact with 14-3-3 proteins in tomato fruit, including sucrose phosphate synthase (SPS; Solyc07g007790 and Solyc09g092130), cytosolic invertase (CINV; Solyc06g065210 and Solyc04g081440) and sucrose synthase (SS; Solyc07g042520 and Solyc07g042550) (Table 7 and Fig. 17). All of these enzymes have previously been identified as 14-3-3 targets. 14-3-3 was found to interact with spinach SPS via the phosphorylated Ser229 residue and to form a complex of inhibited SPS activity[36]. Phylogenetic analysis indicated tomato SPS isoforms, Solyc07g007790 and Solyc09g092130, to be the closest homologues of Arabidopsis SPS1F and SPS3F, I thus assigned them the names SlSPS1F and SlSPS3F, respectively (Fig. 18A). SlSPS1F contains a conserved 14-3-3 binding motif, including Ser221, corresponds to the spinach Ser229, suggesting that the involvement of this motif for the interaction between SPS and 14-3-3 proteins also in tomato fruit (Fig. 19A). In contrast, the Ser221

of SlSPS1F is not conserved in SlSPS3F, even though this protein was also detected as a 14-3-3 interactor in this study. This suggests that the binding of 14-3-3 to SPS occurs at multiple sites rather than a single site and that varies among the SPS isoforms. Indeed, the 14-3-3-Pred database searching found multiple 14-3-3 binding motifs in SlSPS proteins, with one of these, Ser157 of SlSPS3F was highly conserved (Fig. 19B). The 14-3-3 binding motifs of SPS may exhibit variance due to distinct functional regulation of the SPS isoenzymes. The transcriptomic profile of *SlSPS* genes also implies functional differences between the isoforms. Microarray data of The Tomato Genome Consortium (2012)[18], indicated that only the expression of *SlSPS1F* gene , but not of the *SlSPS2F, 3F* and *4F* genes, gradually increases during fruit development in a stage-dependent manner (Fig. 18B to E). Interestingly, Biais et al[37] showed that the total SPS activity decreases as fruit matured, followed by a dramatic increases during later ripening stages, this is not linearly related to the gene expression pattern, thus suggesting that SPS activity is fine-tuned by post-translational regulation, and I posit via interacting with 14-3-3 in tomato fruit. Interactions between CINV and 14-3-3 proteins in Arabidopsis were shown to be phosphorylation-dependent and to be mediated by calcium-dependent protein kinase 3[38]. CINV activity was positively regulated by interactions with 14-3-3 and the levels of hexoses, such as glucose and fructose, were decreased in root tissue of 14-3-3 quadruple mutants[38]. Pull-down proteomic analysis in barley grain showed that SS was also a target of 14-3-3 protein, with the complex of inhibited SS activity[39]. SS activity was reported to be increased in transgenic tomato over-expressing the SPS gene, suggesting that the activities of these enzymes are coordinately regulated in tomato fruit[40]. My results therefore suggest that 14-3-3 proteins contribute to such a regulation.

Carbohydrate metabolism: Cell wall metabolism

Plant cell walls are comprised of large amounts of pectic and hemicellulose polysaccharides, which are mainly derived from sugars and sugar phosphates[41]. During fruit development, the cell wall components change significantly; these changes confer fruit their texture, softeness and shelf-life characteristics. In this study, several 14-3-3 interactors involved in cell wall metabolism were identified in tomato fruit (Table 7). The

alpha-1,4-glucan-protein synthase (Solyc03g114860) displays strong homology to Arabidopsis reversibly glycosylated polypeptide (RGP) proteins. BLAST results showed that the protein sequence of Solyc03g114860 was 89% and 88% identical to that of AtRGP1 and AtRGP3, respectively. The RGP protein family constitute UDP-$_L$-arabinose (UDP-$_L$-Ara) mutases, and the interconversion of UDP-arabinopyranose (UDP-Ara*p*) and UDP-arabinofuranose (UDP-Ara*f*) is essential for cell wall establishment[42]. UDP-$_L$-rhamnose synthase (Solyc10g007480) catalyzes the plant specific synthesis of UDP-$_L$-rhamnose from UDP-glucose[43], and overexpression of this protein in Arabidopsis resulted in an increased rhamnose content of the cell walls[44]. Three UDP-glucose dehydrogenases (Solyc02g067080, Solyc06g069550 and Solyc02g088690) were identified in tomato which catalyzes the formation of UDP-glucuronic acid, a precursor of cell wall components[45]. Sugars derived from UDP-$_L$-Ara, UDP-rhamnose and UDP-glucuronic acid are components of pectic polysaccharides[46], which are increased during cell expansion and undergo modifications during fruit ripening[47]. One of the modifications is the removal of methyl ester groups by pectin methylesterases (PME), two PME proteins encoded by *Solyc03g123630* and *Solyc07g064180* were detected as 14-3-3 interactors in this study. Down regulation of fruit specific PME2 in tomato provoked a higher degree of pectin methylesterification and a lower degree of pectin depolymerization[48]. A glycoside hydrolase, encoded by *Solyc05g009470*, was also identified as 14-3-3 interacting protein; its homologous gene in Arabidopsis, designated *alpha-xylosidase 1*, was shown to encode a protein responsible for the degradation of xyloglucan, a most abundant hemicellulose present in cell walls[49]. Methylenetetrahydrofolate reductase (MTHFR), which converts 5,10-methylenetetrahydrofolate to 5-methyltetrahydrofolate, plays a key role in the methyl cycle, folate metabolism and homocysteine homeostasis[50]. A MTHFR protein encoded by *Solyc11g008870* was also be detected as 14-3-3 interactor in this study. Maize MTHFR was shown to be responsible for the *bm2* mutant, which has a reddish-brown color phenotype and reduced lignin accumulation[51]. Lignin is a critical structural component of cell walls. Three different hydroxycinnamyl alcohol subunits, monolignols *p*-coumaryl, coniferyl and sinapyl alcohol, result in hydroxyphenyl (H-type), guaiacyl (G-type) and syringyl (S-type) lignins, respectively[52]. G-type and S-type lignins can be

synthesized from the S-adenosyl-L-methionine (SAM), produced from the MTHFR product 5-methyltetrahydrofolate. Finally, the Solyc02g077880 protein was identified in this study. It was predicted to be a candidate related to the firmness phenotype of tomato fruit though the quantitative trait locus analysis, although the detailed function of this protein has not been determined[53]. Several enzymes detected in this study, such as alpha-1,4-glucan-protein synthase (Solyc03g114860), UDP-L-rhamnose synthase (Solyc10g007480) and methylenetetrahydrofolate reductase (Solyc11g008870), were not detected in previous 14-3-3 interactome analyses using Arabidopsis[7,54,55]. Taken together, it seems reasonable to speculate that the 14-3-3 regulation of these enzymes involved in cell wall metabolism may contribute to fruit texture, softeness and shelf-life characteristics.

Carbohydrate metabolism: Other carbohydrate metabolism

In addition to the enzymes directly involved in sucrose metabolism, this study also identified several other carbohydrate metabolism related enzymes that bind to 14-3-3 proteins. These include starch phosphorylase (PHS; Solyc05g012510), phosphofructokinase (PFP; Solyc12g095760), fructose 1,6-bisphosphate aldolase (FBA; Solyc01g110360.), glyceraldehyde 3-phosphate dehydrogenase (GAPDH; Solyc04g009030), phospho*enol*pyruvate carboxylase (PEPC; Solyc12g014250), trehalose 6-phosphate synthase (TPS; Solyc08g076650) and proteins constituting the heterometric plastid acetyl-CoA carboxylase (ACCase; Solyc01g008330, Solyc09g013080 and Solyc01g007340) (Table 7 and Fig. 17). PHS, a plastid alpha-glucan phosphorylase, which catalyzes the reversible transfer of glucosyl units from glucose 1-phosphate to alpha-1,4-linked glucans. Although the physiological connection between plastid PHS and starch mobilization remains unclear[56], double knockout mutants of *phs1* and a related enzyme showed that PHS1 is involved in starch metabolism in the dark and indirectly prevents induction of chloroplast disintegration[57]. Arabidopsis single *phs1* mutant exhibited white lesions under abiotic stress conditions such as drought or salinity, suggesting that PHS involved in abiotic stress tolerance[58]. During tomato fruit development, PHS activity is maintained at a similar levels, and is therefore unlikely to be associated with the reduction in the amount of starch[59]. Further

study is required to determine whether, in tomato fruit, PHS, together with 14-3-3 proteins, is involved in starch mobilization during ripening or has a regulatory role in environmental stress responses. PFP catalyzes reversible reactions that use pyrophosphate as a phosphate donor and converts fructose 6-phosphate to fructose 1,6-phosphate[60]. FBA, which catalyzes the cleavage of fructose 1,6-bisphosphate into glyceraldehyde 3-phosphate and dihydroxyacetone phosphate (DHAP) or the reverse condensation reaction, is involved in glycolysis, gluconeogenesis and the Calvin cycle[61]. Tomato FBA (Solyc01g110360) is homologous to the Arabidopsis FBA protein, AtFBA2 (At4g38970). AtFBA2 is a plastid class I FBA protein, with an *fba2* mutant showing growth inhibition and reduced starch accumulation[62]. GAPDH catalyzes the reversible conversion of glyceraldehyde 3-phosphate to 1,3-bisphosphoglycerate and may also be involved in reactive oxygen species autophagy, plant immune response and viable pollen development in Arabidopsis[63,64]. PEPC catalyzes the irreversible β-carboxylation of PEP to form oxaloacetate and P_i[65]. PEPC plays a central role of glycolysis, respiration and photosynthate partitioning[66], as well as being an important route for carbon dioxide fixation particularly in C4 plants. A tomato fruit specific PEPC isoenzyme was shown to be related to the accumulation of malate and citrate, which were responsible for the turgor force derived rapid cell expansion[67]. TPS catalyzes the formation of trehalose 6-phosphate (T6P) from glucose 6-phosphate and UDP-glucose and is key step in trehalose synthesis[68]. T6P is an important signaling molecular that regulates many aspects of plant growth and development, particularly via sugar mediated metabolic and signaling pathways[69,70]. I identified Solyc08g076650, which is a homologous protein to AtTPS5. AtTPS5 is phosphorylated by Snf1-related protein kinase 1 (SnRK1) at Ser21 and Thr48, both of which mediate 14-3-3 binding to AtTPS5[71]. ACCase catalyzes the formation of malonyl-CoA from acetyl-CoA that is produced by pyruvate dehydrogenase, with this reaction considered the committing step of fatty acid synthesis pathway[72,73]. The plastidial heteromeric form of ACCase comprises biotin carboxylase (Solyc01g008330), biotin carboxyl carrier protein, carboxyltransferase α subunit (Solyc09g013080) and carboxyltransferase β subunit (Solyc01g007340)[72]. With the exception of the biotin carboxyl carrier protein, the rest of these proteins were identified as 14-3-3 interacting proteins in this study (Table 7).

Overexpression of the Arabidopsis cytosolic homomeric *ACC1* gene containing chloroplast localization signaling sequences in potato increased fatty acid synthesis and enhanced the amount of triacylglycerol production more than five-fold[74]. GAPDH, PEPC and ACCase proteins were identified as 14-3-3 interacting proteins in previous MS analysis using Arabidopsis[7,15,75]. My 14-3-3 binding site prediction found that, with the exception of PFP, all other enzymes sequences contained high confidence 14-3-3 binding sites (Table 7). Taken together, these results suggest 14-3-3 proteins may participate in the regulation of glycolysis, respiration, photosynthate partitioning and fatty acid synthesis, as well as in the indirect regulation of sucrose and hexose homeostasis in tomato fruit.

Photosynthesis

Photosynthesis in fruit has been the focus of considerable research effort. Tomato fruit develops from a non-photosynthetic tissue (fertilization) to a photosynthetic tissue (cell division and cell expansion) and then revert to a non-photosynthetic tissue again (ripening). Although the net photosynthesis in fruit during development is zero, gross photosynthesis (which includes re-assimilation of respiratory CO_2) is active and may even reach comparable rates to those observed in the leaf[76,77]. Alternatively, whilst fruit photosynthesis is seemingly unimportant for tomato fruit development, it may regulate the formation of seeds[78]. Moreover, a proteomic analysis of different development stages of tomato fruit showed that, Rubisco is present in even fully developed red fruit[79]. These observations are consistent with the finding showed the maintenance of the ratio of Rubisco oxygenase activity to Rubisco carboxylase activity during tomato fruit ripening[76]. This is in agreement with the hypothesis that Rubisco re-assimilates respiratory CO_2 in fruit by consuming the reducing power produced by the pentose phosphate pathway. Interestingly, the enzyme catalyzing the first step of the pentose phosphate pathway, glucose 6-phosphate dehydrogenase (G6PDH; Solyc07g045540), was also found to be interact with 14-3-3, suggested the involvement of 14-3-3 regulation in this process (Table 7). G6PDH activity was shown to be very high in chloroplasts and chromoplasts, suggesting that this high activity may maintain the non-photosynthetic production of reducing power[80]. This study identified the Rubisco small

chain (Solyc02g063150), two Rubisco activases (Solyc09g011080 and Solyc10g086580), six chlorophyll *a/b* binding proteins (Solyc02g070940, Solyc01g105030, Solyc10g007690, Solyc07g063600, Solyc07g047850 and Solyc03g115900), and oxygen-evolving enhancer protein 1 of photosystem II (Solyc02g065400) as 14-3-3 interactors (Table 7). Rubisco activase belongs to the AAA+ family of chaperone-like function proteins. Interactions of these proteins with Rubisco provoke a conformational changes in the later, releasing inhibitory sugar-phosphates from its active site by the consuming of ATP[81]. Chlorophyll *a/b* binding proteins in Arabidopsis belong to the Lhcb and Lhca families. Lhcb1, Lhcb2, and Lhcb3 form light-harvesting complex II (LHCII); Lhcb4, Lhcb5 and Lhcb6 are associated with photosystem II (PSII); and the Lhcas make up the antenna of photosystem I (PSI)[82]. BLAST analysis using the Arabidopsis protein database (TAIR10) identified putative tomato proteins homologous to Arabidopsis Lhcb1 (Solyc02g070940), Lhcb2 (Solyc07g047850), Lhcb3 (Solyc07g063600) and Lhcb6 (Solyc01g105030) to form the LHCII; and proteins homologous to Arabidopsis Lhca3 (Solyc10g007690) and Lhca4 (Solyc03g115900) to form the antenna of PSI (Table 6). Besides the core complex of PSII and PSI, four lumen-exposed extrinsic proteins constitute the oxygen-evolving complex for optimal oxygen evolution[83]. The homolog of one of these proteins, oxygen-evolving enhancer protein 1 of photosystem II (Solyc02g065400), called PsbO1/2 in Arabidopsis, was identified as 14-3-3 interacting protein in this study (Table 7). T-DNA insertion knockout mutant analyses in Arabidopsis revealed the roles of PsbOs in photosynthesis[84]. When taken together, my results suggest that 14-3-3 proteins may participate in the regulation of photosynthesis in tomato fruit.

Reference

1. Obsil, T. & Obsilova, V. Structural basis of 14-3-3 protein functions. *Semin. Cell Dev. Biol.* **22,** 663–72 (2011).
2. Roberts, M. R. 14-3-3 Proteins find new partners in plant cell signalling. *Trends Plant Sci.* **8,** 218–223 (2003).
3. Chevalier, D., Morris, E. R. & Walker, J. C. 14-3-3 and FHA domains mediate phosphoprotein interactions. *Annu. Rev. Plant Biol.* **60,** 67–91 (2009).
4. Denison, F. C., Paul, A.-L., Zupanska, A. K. & Ferl, R. J. 14-3-3 Proteins in Plant Physiology. *Semin. Cell Dev. Biol.* **22,** 720–727 (2011).
5. Comparot, S., Lingiah, G. & Martin, T. Function and specificity of 14-3-3 proteins in the regulation of carbohydrate and nitrogen metabolism. *J. Exp. Bot.* **54,** 595–604 (2003).
6. Oecking, C. & Jaspert, N. Plant 14-3-3 proteins catch up with their mammalian orthologs. *Curr. Opin. Plant Biol.* **12,** 760–765 (2009).
7. Chang, I.-F. *et al.* Proteomic profiling of tandem affinity purified 14-3-3 protein complexes in *Arabidopsis thaliana*. *Proteomics* **9,** 2967–2985 (2009).
8. Sato, T. *et al.* Identification of 14-3-3 proteins as a target of ATL31 ubiquitin ligase, a regulator of the C/N response in Arabidopsis. *Plant J.* **68,** 137–46 (2011).
9. Coruzzi, G. M. & Zhou, L. Carbon and nitrogen sensing and signaling in plants: emerging 'matrix effects'. *Curr. Opin. Plant Biol.* **4,** 247–53 (2001).
10. Aoyama, S. *et al.* Ubiquitin ligase ATL31 functions in leaf senescence in response to the balance between atmospheric CO_2 and nitrogen availability in arabidopsis. *Plant Cell Physiol.* **55,** 293–305 (2014).
11. Lu, Y. *et al.* ABI1 regulates carbon/nitrogen-nutrient signal transduction independent of ABA biosynthesis and canonical ABA signalling pathways in Arabidopsis. *J. Exp. Bot.* **66,** 2763–2771 (2015).
12. Sato, T. *et al.* CNI1/ATL31, a RING-type ubiquitin ligase that functions in the carbon/nitrogen response for growth phase transition in Arabidopsis seedlings. *Plant J.* **60,** 852–64 (2009).
13. Aguilar-Hernández, V., Aguilar-Henonin, L. & Guzmán, P. Diversity in the Architecture of ATLs, a Family of Plant Ubiquitin-Ligases, Leads to Recognition

and Targeting of Substrates in Different Cellular Environments. *PLoS One* **6,** e23934 (2011).

14. Yasuda, S. *et al.* Phosphorylation of arabidopsis ubiquitin ligase ATL31 is critical for plant carbon/nitrogen nutrient balance response and controls the stability of 14-3-3 proteins. *J. Biol. Chem.* **289,** 15179–15193 (2014).
15. Cotelle, V. *et al.* 14-3-3s regulate global cleavage of their diverse binding partners in sugar-starved Arabidopsis cells. *EMBO J.* **19,** 2869–2876 (2000).
16. Tohge, T., Alseekh, S. & Fernie, A. R. On the regulation and function of secondary metabolism during fruit development and ripening. *J. Exp. Bot.* **65,** 4599–4611 (2014).
17. Shikata, M. *et al.* TOMATOMA Update: Phenotypic and Metabolite Information in the Micro-Tom Mutant Resource. *Plant Cell Physiol.* **0,** pcv194 (2015).
18. Tomato, T. & Consortium, G. The tomato genome sequence provides insights into fleshy fruit evolution. *Nature* **485,** 635–41 (2012).
19. Pate, J. S., Sharkey, P. J. & Atkins, C. A. Nutrition of a developing legume fruit: functional economy in terms of carbon, nitrogen, water. *Plant Physiol.* **59,** 506–10 (1977).
20. Teper, D. *et al. Xanthomonas euvesicatoria* type III effector XopQ interacts with tomato and pepper 14-3-3 isoforms to suppress effector-triggered immunity. *Plant J.* **77,** 297–309 (2014).
21. Oh, C.-S. & Martin, G. B. Tomato 14-3-3 Protein TFT7 Interacts with a MAP Kinase Kinase to Regulate Immunity-associated Programmed Cell Death Mediated by Diverse Disease Resistance Proteins. *J. Biol. Chem.* **286,** 14129–14136 (2011).
22. XU, W., SHI, W., JIA, L., LIANG, J. & ZHANG, J. TFT6 and TFT7, two different members of tomato 14-3-3 gene family, play distinct roles in plant adaption to low phosphorus stress. *Plant. Cell Environ.* **35,** 1393–1406 (2012).
23. Xu, W. *et al.* The Tomato 14-3-3 protein TFT4 modulates H+ efflux, basipetal auxin transport, and the PKS5-J3 pathway in the root growth response to alkaline stress. *Plant Physiol.* **163,** 1817–28 (2013).
24. Scott, J. W. & Harbaugh, B. K. MicroeTom. A Miniature Dwarf Tomato.

Agricultural Experiment Station. *Inst. Food Agric. Sci. Univ. Florida Circ.* **S370,** 1–6 (1989).

25. Tsunoda, Y. *et al.* Improving expression and solubility of rice proteins produced as fusion proteins in Escherichia coli. *Protein Expr. Purif.* **42,** 268–277 (2005).
26. Nakagawa, T. *et al.* Development of series of gateway binary vectors, pGWBs, for realizing efficient construction of fusion genes for plant transformation. *J. Biosci. Bioeng.* **104,** 34–41 (2007).
27. Sun, H.-J., Uchii, S., Watanabe, S. & Ezura, H. A highly efficient transformation protocol for Micro-Tom, a model cultivar for tomato functional genomics. *Plant Cell Physiol.* **47,** 426–31 (2006).
28. Murashige, T. & Skoog, F. A Revised Medium for Rapid Growth and Bio Assays with Tobacco Tissue Cultures. *Physiol. Plant.* **15,** 473–497 (1962).
29. Madeira, F. *et al.* 14-3-3-Pred: improved methods to predict 14-3-3-binding phosphopeptides. *Bioinformatics* **31,** 2276–2283 (2015).
30. Takai, R. *et al.* EL5, a rice N-acetylchitooligosaccharide elicitor-responsive RING-H2 finger protein, is a ubiquitin ligase which functions in vitro in co-operation with an elicitor-responsive ubiquitin-conjugating enzyme, OsUBC5b. *Plant J.* **30,** 447–455 (2002).
31. Oh, C.-S. Characteristics of 14-3-3 Proteins and Their Role in Plant Immunity. *Plant Pathol. J.* **26,** 1–7 (2010).
32. Tang, X. *et al.* Ubiquitin-conjugated degradation of golden 2-like transcription factor is mediated by CUL4-DDB1-based E3 ligase complex in tomato. *New Phytol.* **209,** 1028–39 (2016).
33. Powell, A. L. T. *et al.* Uniform ripening encodes a Golden 2-like transcription factor regulating tomato fruit chloroplast development. *Science* **336,** 1711–5 (2012).
34. de Boer, A. H., van Kleeff, P. J. M. & Gao, J. Plant 14-3-3 proteins as spiders in a web of phosphorylation. *Protoplasma* **250,** 425–440 (2013).
35. Johnson, C. *et al.* Bioinformatic and experimental survey of 14-3-3-binding sites. *Biochem. J.* **427,** 69–78 (2010).
36. Toroser, D., Athwal, G. S. & Huber, S. C. Site-specific regulatory interaction

between spinach leaf sucrose-phosphate synthase and 14-3-3 proteins. *FEBS Lett.* **435,** 110–114 (1998).

37. Biais, B. *et al.* Remarkable Reproducibility of Enzyme Activity Profiles in Tomato Fruits Grown under Contrasting Environments Provides a Roadmap for Studies of Fruit Metabolism. *Plant Physiol.* **164,** 1204–1221 (2014).
38. Gao, J. *et al.* Light modulated activity of root alkaline/neutral invertase involves the interaction with 14-3-3 proteins. *Plant J.* 785–796 (2014). doi:10.1111/tpj.12677
39. Alexander, R. D. & Morris, P. C. A proteomic analysis of 14-3-3 binding proteins from developing barley grains. *Proteomics* **6,** 1886–1896 (2006).
40. Nguyen-Quoc, B., N'Tchobo, H., Foyer, C. H. & Yelle, S. Overexpression of sucrose phosphate synthase increases sucrose unloading in transformed tomato fruit. *J. Exp. Bot.* **50,** 785–791 (1999).
41. Carrari, F. Metabolic regulation underlying tomato fruit development. *J. Exp. Bot.* **57,** 1883–1897 (2006).
42. Rautengarten, C. *et al.* The Interconversion of UDP-Arabinopyranose and UDP-Arabinofuranose Is Indispensable for Plant Development in Arabidopsis. *Plant Cell* **23,** 1373–1390 (2011).
43. Oka, T., Nemoto, T. & Jigami, Y. Functional Analysis of Arabidopsis thaliana RHM2/MUM4, a Multidomain Protein Involved in UDP-D-glucose to UDP-L-rhamnose Conversion. *J. Biol. Chem.* **282,** 5389–5403 (2007).
44. Wang, J. *et al.* Overexpression of a cytosol-localized rhamnose biosynthesis protein encoded by Arabidopsis RHM1 gene increases rhamnose content in cell wall. *Plant Physiol. Biochem.* **47,** 86–93 (2009).
45. Reboul, R. *et al.* Down-regulation of UDP-glucuronic Acid Biosynthesis Leads to Swollen Plant Cell Walls and Severe Developmental Defects Associated with Changes in Pectic Polysaccharides. *J. Biol. Chem.* **286,** 39982–39992 (2011).
46. Orfila, C. *et al.* Altered cell wall disassembly during ripening of Cnr tomato fruit: Implications for cell adhesion and fruit softening. *Planta* **215,** 440–447 (2002).
47. Lunn, D., Phan, T. D., Tucker, G. a. & Lycett, G. W. Cell wall composition of tomato fruit changes during development and inhibition of vesicle trafficking is

associated with reduced pectin levels and reduced softening. *Plant Physiol. Biochem.* **66,** 91–97 (2013).

48. Tieman, D. M., Harriman, R. W., Ramamohan, G. & Handa, A. K. An Antisense Pectin Methylesterase Gene Alters Pectin Chemistry and Soluble Solids in Tomato Fruit. *Plant Cell* **4,** 667–679 (1992).
49. Günl, M. & Pauly, M. AXY3 encodes a α-xylosidase that impacts the structure and accessibility of the hemicellulose xyloglucan in Arabidopsis plant cell walls. *Planta* **233,** 707–719 (2011).
50. Vickers, T. J. *et al.* Biochemical and genetic analysis of methylenetetrahydrofolate reductase in Leishmania metabolism and virulence. *J. Biol. Chem.* **281,** 38150–8 (2006).
51. Tang, H. M. *et al.* The maize brown midrib2 (bm2) gene encodes a methylenetetrahydrofolate reductase that contributes to lignin accumulation. *Plant J.* **77,** 380–392 (2014).
52. Barros, J., Serk, H., Granlund, I. & Pesquet, E. The cell biology of lignification in higher plants. *Ann. Bot.* **115,** 1053–1074 (2015).
53. Chapman, N. H. *et al.* High-Resolution Mapping of a Fruit Firmness-Related Quantitative Trait Locus in Tomato Reveals Epistatic Interactions Associated with a Complex Combinatorial Locus. *Plant Physiol.* **159,** 1644–1657 (2012).
54. Paul, A.-L. *et al.* Comparative interactomics: analysis of arabidopsis 14-3-3 complexes reveals highly conserved 14-3-3 interactions between humans and plants. *J. Proteome Res.* **8,** 1913–24 (2009).
55. Swatek, K. N., Graham, K., Agrawal, G. K. & Thelen, J. J. The 14-3-3 isoforms chi and epsilon differentially bind client proteins from developing Arabidopsis seed. *J. Proteome Res.* **10,** 4076–4087 (2011).
56. Zeeman, S. C., Smith, S. M. & Smith, A. M. The breakdown of starch in leaves. *New Phytol.* **163,** 247–261 (2004).
57. Malinova, I. *et al.* Double Knockout Mutants of Arabidopsis Grown under Normal Conditions Reveal that the Plastidial Phosphorylase Isozyme Participates in Transitory Starch Metabolism. *Plant Physiol.* **164,** 907–921 (2014).
58. Zeeman, S. C. *et al.* Plastidial alpha-glucan phosphorylase is not required for

starch degradation in Arabidopsis leaves but has a role in the tolerance of abiotic stress. *Plant Physiol.* **135,** 849–58 (2004).

59. Robinson, N. L., Hewitt, J. D. & Bennett, A. B. Sink metabolism in tomato fruit : I. Developmental changes in carbohydrate metabolizing enzymes. *Plant Physiol.* **87,** 727–30 (1988).
60. Reeves, R. E., South, D. J., Blytt, H. J. & Warren, L. G. Pyrophosphate:D-fructose 6-phosphate 1-phosphotransferase. A new enzyme with the glycolytic function of 6-phosphofructokinase. *J. Biol. Chem.* **249,** 7737–41 (1974).
61. Shams, F., Oldfield, N. J., Wooldridge, K. G. & Turner, D. P. J. Fructose-1,6-bisphosphate aldolase (FBA)–a conserved glycolytic enzyme with virulence functions in bacteria: 'ill met by moonlight'. *Biochem. Soc. Trans.* **42,** 1792–1795 (2014).
62. Lu, W. *et al.* Identification and characterization of fructose 1,6-bisphosphate aldolase genes in Arabidopsis reveal a gene family with diverse responses to abiotic stresses. *Gene* **503,** 65–74 (2012).
63. Henry, E., Fung, N., Liu, J., Drakakaki, G. & Coaker, G. Beyond Glycolysis: GAPDHs Are Multi-functional Enzymes Involved in Regulation of ROS, Autophagy, and Plant Immune Responses. *PLOS Genet.* **11,** e1005199 (2015).
64. Munoz-Bertomeu, J. *et al.* The Plastidial Glyceraldehyde-3-Phosphate Dehydrogenase Is Critical for Viable Pollen Development in Arabidopsis. *Plant Physiol.* **152,** 1830–1841 (2010).
65. Chollet, R., Vidal, J. & O'Leary, M. H. PHOSPHOENOLPYRUVATE CARBOXYLASE: A Ubiquitous, Highly Regulated Enzyme in Plants. *Annu. Rev. Plant Physiol. Plant Mol. Biol.* **47,** 273–298 (1996).
66. O'Leary, B., Park, J. & Plaxton, W. C. The remarkable diversity of plant PEPC (phosphoenolpyruvate carboxylase): recent insights into the physiological functions and post-translational controls of non-photosynthetic PEPCs. *Biochem. J.* **436,** 15–34 (2011).
67. Guillet, C. *et al.* A fruit-specific phospho enolpyruvate carboxylase is related to rapid growth of tomato fruit. *Planta* **214,** 717–26 (2002).
68. Eastmond, P. J. & Graham, I. A. Trehalose metabolism: a regulatory role for

trehalose-6-phosphate? *Curr. Opin. Plant Biol.* **6,** 231–235 (2003).

69. Tsai, A. Y.-L. & Gazzarrini, S. Trehalose-6-phosphate and SnRK1 kinases in plant development and signaling: the emerging picture. *Front. Plant Sci.* **5,** 119 (2014).
70. Yadav, U. P. *et al.* The sucrose-trehalose 6-phosphate (Tre6P) nexus: Specificity and mechanisms of sucrose signalling by. *J. Exp. Bot.* **65,** 1051–1068 (2014).
71. Harthill, J. E. *et al.* Phosphorylation and 14-3-3 binding of Arabidopsis trehalose-phosphate synthase 5 in response to 2-deoxyglucose. *Plant J.* **47,** 211–23 (2006).
72. Sasaki, Y. & Nagano, Y. Plant acetyl-CoA carboxylase: structure, biosynthesis, regulation, and gene manipulation for plant breeding. *Biosci. Biotechnol. Biochem.* **68,** 1175–1184 (2004).
73. Chou, C. Y., Yu, L. P. C. & Tong, L. Crystal structure of biotin carboxylase in complex with substrates and implications for its catalytic mechanism. *J. Biol. Chem.* **284,** 11690–11697 (2009).
74. Klaus, D., Ohlrogge, J. B., Neuhaus, H. E. & Dörmann, P. Increased fatty acid production in potato by engineering of acetyl-CoA carboxylase. *Planta* **219,** 389–396 (2004).
75. Shin, R., Jez, J. M., Basra, A., Zhang, B. & Schachtman, D. P. 14-3-3 Proteins fine-tune plant nutrient metabolism. *FEBS Lett.* **585,** 143–147 (2011).
76. Bravdo, B. A., Palgi, A. & Lurie, S. Changing ribulose diphosphate carboxylase/oxygenase activity in ripening tomato fruit. *Plant Physiol.* **60,** 309–12 (1977).
77. Carrara, S., Pardossi, A., Soldatini, G. F., Tognoni, F. & Guidi, L. Photosynthetic activity of ripening tomato fruit. *Photosynthetica* **39,** 75–78 (2001).
78. Lytovchenko, A. *et al.* Tomato Fruit Photosynthesis Is Seemingly Unimportant in Primary Metabolism and Ripening But Plays a Considerable Role in Seed Development. *Plant Physiol.* **157,** 1650–1663 (2011).
79. Suzuki, M. *et al.* Plastid Proteomic Analysis in Tomato Fruit Development. *PLoS One* **10,** e0137266 (2015).
80. Aoki, K., Yamamoto, M. & Wada, K. Photosynthetic and heterotrophic ferredoxin isoproteins are colocalized in fruit plastids of tomato. *Plant Physiol.* **118,** 439–49 (1998).

81. Portis, A. R., Li, C., Wang, D. & Salvucci, M. E. Regulation of Rubisco activase and its interaction with Rubisco. *J. Exp. Bot.* **59,** 1597–1604 (2008).
82. Pietrzykowska, M. *et al.* The Light-Harvesting Chlorophyll a/b Binding Proteins Lhcb1 and Lhcb2 Play Complementary Roles during State Transitions in Arabidopsis. *Plant Cell* **26,** 3646–3660 (2014).
83. Allahverdiyeva, Y. *et al.* Arabidopsis plants lacking PsbQ and PsbR subunits of the oxygen-evolving complex show altered PSII super-complex organization and short-term adaptive mechanisms. *Plant J.* **75,** 671–684 (2013).
84. Murakami, R. *et al.* Functional dissection of two Arabidopsis PsbO proteins PsbO1 and PsbO2. *FEBS J.* **272,** 2165–2175 (2005).

Table 4. Primers used for plasmid constructs.

Gene	Froward	Reverse
SlATL31ΔTM	CACCATGACTGCTGCTGCTAC	TCGGCTCGATCTCCGGTTTAA
SlATL31ΔTM Mutagenesis*	ATCCCTAAG**TCT**GATCACGTTTTTCAT	ATGAAAAACGTGATC**AGA**CTTAGGGAT
SlTFT3	CACCATGGCAGTAGCACCAA	GAAGATCCCAAACCTGAAGAAAAAAAT
SlTFT10	CACCATGGCAGCTCTAATTCCT	GAAACCCGACAATGAACAACAG

* Nucleotides marked in bold are the mutation sites at Cys138 of SlATL31

Table 5. Arabidopsis 14-3-3λ protein identified by MS/MS analysis.

# Rep.[a]	AGI accession[b]	Protein description	Score[c]	Coverage (%)	MW[d]	Unique peptides[d]
1	At5G10450	14-3-3*λ* (GRF6)	942	60.1	31	12
2	At5G10450	14-3-3*λ* (GRF6)	827	61.5	31	16
3	At5G10450	14-3-3*λ* (GRF6)	879	60.1	31	14

[a] Number of experimental replications for affinity purification of 14-3-3 complex
[b] Accession number of *Arabidopsis thaliana* gene in the TAIR10 database
[c] The score assigned by SEQUEST software after database searching
[d] Theatrical molecular weight of the identified protein
[e] Total number of detected unique peptides of the identified protein

Table 6. TFT isoforms in 14-3-3 complexes identified by MS/MS analysis.

ITAG accession[a]	Protein description	Score[b]	Coverage (%)	MW[c]	Unique peptides[d]
Solyc04g012120	TFT5	272	67.7	28.8	4
Solyc12g057110	TFT2	260	53.5	28.9	7
Solyc11g010200	TFT6	262	52.8	30.6	2
Solyc04g074510	TFT3	256	48.8	30.4	5
Solyc03g034180	TFT11	222	35.8	29.1	1
Solyc04g074230	TFT7	192	37.7	30.6	4
Solyc12g010860	TFT8	45	14.0	29.5	2

[a] ITAG accession number of *Solanum lycopersicum* genes
[b] The score assigned by SEQUEST software after database searching
[c] Theoritical molecular weight of the identified protein
[d] Total number of detected unique peptides of the identified protein

Table 7. Putative 14-3-3 interacting proteins identified by MS/MS analysis.

ITAG accession[a]	Protein description	Score[b]	Coverage (%)	MW[c]	Unique peptides[d]	14-3-3 motif[e]
Carbon metabolism						
Solyc01g008330	Acetyl-CoA carboxylase biotin carboxylase	12	10.1	58.5	3	-
Solyc09g013080	Acetyl-CoA carboxylase carboxyl transferase alpha subunit	30	18.9	84.8	8	+
Solyc01g007340	Acetyl-CoA carboxylase carboxyl transferase beta subunit	27	17.7	57.6	7	-
Solyc08g076650	Trehalose 6-phosphate synthase	13	7.7	97.2	4	+
Solyc01g110360	Fructose-bisphosphate aldolase	15	13.7	42.7	1	+
Solyc04g009030	Glyceraldehyde 3-phosphate dehydrogenase	19	22.5	42.7	4	+
Solyc06g065210	Cytosolic invertase	20	8.3	62.7	2	+
Solyc04g081440	Cytosolic invertase	38	19.1	65.2	5	+
Solyc12g014250	Phospho*enol*pyruvate carboxylase	82	29.0	110.1	9	+
Solyc05g012510	Starch phosphorylase	14	7.4	109.8	4	+
Solyc12g095760	Pyrophosphate-dependent phosphofructokinase PfpB	26	14.1	67.2	6	-
Solyc09g092130	Sucrose phosphate synthase	39	15.7	119.5	9	+
Solyc07g007790	Sucrose phosphate synthase	116	23.5	118.4	22	+
Solyc07g042520	Sucrose synthase	25	14.4	91.6	6	+
Solyc07g042550	Sucrose synthase	57	18.9	92.5	2	+
Cell wall metabolism						
Solyc03g114860	Alpha-1 4-glucan-protein synthase	27	22.0	40.1	1	-
Solyc10g007480	UDP-$_{L}$-rhamnose synthase	21	11.5	66.3	4	-
Solyc05g009470	Glycoside hydrolase, family 31	18	7.7	104.6	5	+
Solyc11g008870	Methylenetetrahydrofolate reductase	33	13.7	67.2	5	-
Solyc03g123630	Pectinesterase	14	9.8	64.0	4	+
Solyc07g064180	Pectinesterase	29	13.7	60.5	2	+
Solyc02g067080	UDP-$_{D}$-glucose dehydrogenase	13	9.5	56.6	3	+
Solyc06g069550	UDP-$_{D}$-glucose dehydrogenase	14	10.2	52.9	1	+
Solyc02g088690	UDP-glucose 6-dehydrogenase	15	11.1	34.3	1	+
Solyc02g077880	Auxin-repressed protein	23	48.2	13.4	4	+
Photosynthesis & pentose phosphate pathway						
Solyc02g070940	Chlorophyll *a/b* binding protein	51	44.2	28.1	3	-
Solyc01g105030	Chlorophyll *a/b* binding protein	14	20.8	27.2	3	-
Solyc10g007690	Chlorophyll *a/b* binding protein	20	25.4	29.3	3	+
Solyc07g063600	Chlorophyll *a/b* binding protein	30	10.7	28.4	1	-

ITAG accession[a]	Protein description	Score[b]	Coverage (%)	MW[c]	Unique peptides[d]	14-3-3 motif[e]
Solyc07g047850	Chlorophyll *a/b* binding protein	40	27.7	28.8	2	+
Solyc03g115900	Chlorophyll *a/b* binding protein P4	12	17.9	27.8	2	-
Solyc02g065400	Oxygen-evolving enhancer protein 1 of photosystem II	14	26.4	34.9	4	-
Solyc02g063150	Ribulose bisphosphate carboxylase small chain	22	40.7	20.3	2	-
Solyc09g011080	Ribulose-1 5-bisphosphate carboxylase_oxygenase activase	66	40.2	48.6	2	-
Solyc10g086580	Ribulose-1 5-bisphosphate carboxylase_oxygenase activase	81	44.8	49.2	3	-
Solyc07g045540	Glucose-6-phosphate 1-dehydrogenase	20	8.8	65.7	5	+
Amino acid metabolism						
Solyc08g065220	Glycine dehydrogenase P protein	10	4.2	113.0	4	+
Solyc06g073310	Ribosomal L9-like protein	13	28.4	21.9	2	-
Solyc06g019170	Gamma-glutamyl phosphate reductase	17	10.9	77.4	4	+
Protein metabolism						
Solyc01g109940	26S protease regulatory subunit	21	17.8	44.7	5	+
Solyc01g099760	26S protease regulatory subunit 6A homolog	26	19.1	47.5	4	+
Solyc06g082630	26S protease regulatory subunit 6B	16	12.6	46.6	3	+
Solyc10g084050	26S protease regulatory subunit 6B homolog	35	18.4	89.7	1	+
Solyc11g069720	26S protease regulatory subunit 6B homolog	41	18.6	89.5	1	+
Solyc05g018570	26S protease regulatory subunit 8 homolog A	14	11.5	47.0	2	+
Solyc05g013030	26S proteasome regulatory subunit	16	12.3	47.0	4	-
Solyc08g062630	Aminopeptidase-like protein	26	14.1	99.1	8	+
Solyc10g054910	Peptidyl-prolyl cis-trans isomerase	23	14.3	17.9	1	-
Solyc01g087850	Subtilisin-like protease	14	4.8	82.2	3	+
RNA synthesis/processing/regulation						
Solyc05g047520	ATP-dependent RNA helicase DOB1	10	2.4	105.2	2	+
Solyc09g090520	Heterogeneous nuclear ribonucleoprotein A3	10	10.0	47.8	3	-
Solyc12g095960	Insulin-like growth factor 2 mRNA-binding protein	16	17.8	30.4	4	-
Solyc07g045240	RNA-binding protein-like	17	17.6	36.4	4	-
Solyc06g084310	Small nuclear ribonucleoprotein Sm D1	18	39.8	12.6	3	-
Solyc05g049950	Small nuclear ribonucleoprotein-associated protein B	19	19.8	29.6	3	-
Solyc02g085420	U1 small nuclear ribonucleoprotein	52	21.6	56.9	9	+
Solyc09g075200	U1 small nuclear ribonucleoprotein A	19	19.0	28.0	4	-
Chaperone						
Solyc09g091180	Chaperonin Cpn60	11	10.5	61.5	4	+
Solyc09g010630	Heat shock protein 70	72	28.9	71.2	2	+

ITAG accession[a]	Protein description	Score[b]	Coverage (%)	MW[c]	Unique peptides[d]	14-3-3 motif[e]
Solyc07g065840	Heat shock protein 90	81	27.3	80.1	2	+
Solyc06g036290	Heat shock protein 90 (Fragment)	38	15.8	70.2	2	+
Solyc05g010670	Heat shock protein Hsp90	15	7.5	89.7	3	+
Solyc01g090750	T-complex protein 1 subunit alpha	10	5.0	59.2	2	-
Solyc05g056310	T-complex protein 1 subunit gamma	10	6.6	60.7	3	+
Solyc02g063090	T-complex protein 1 subunit zeta	13	8.7	58.8	3	+
Solyc06g065520	T-complex protein eta subunit	21	16.9	60.1	5	+
Solyc01g088080	T-complex protein theta subunit	37	29.0	58.4	10	+
Cytoskeleton						
Solyc04g082560	Actin cytoskeleton-regulatory complex protein PAN1	12	3.7	134.6	3	+
Solyc10g085020	Tubulin beta chain	117	45.3	51.1	2	+
Signaling						
Solyc01g097520	Annexin 11	11	10.9	36.4	4	-
Solyc05g008470	F-box family protein	44	7.5	133.5	2	+
Solyc01g005870	LRR receptor-like serine_threonine-protein kinase, RLP	19	2.4	89.4	1	+
Solyc08g083040	Serine_threonine protein kinase	16	8.9	80.8	4	+
Solyc08g008550	Serine_threonine protein kinase	18	10.9	78.9	4	+
Tetrapyrrole biosynthesis						
Solyc04g009200	Glutamate-1-semialdehyde-2 1-aminomutase	32	18.8	51.5	7	+
Traffic						
Solyc01g079540	ADP-ribosylation factor-like protein 3	12	24.5	21.9	3	-
Solyc06g050770	Alpha-soluble NSF attachment protein	16	22.1	32.5	5	-
Solyc05g052510	Clathrin heavy chain	56	14.2	192.8	2	+
Solyc07g032100	Coatomer alpha subunit-like protein	30	10.2	136.8	2	+
Solyc10g081920	Coatomer subunit beta-1	11	4.9	101.7	2	+
Solyc03g095410	Exocyst complex component protein	13	6.6	90.3	1	+
Solyc04g054470	Myosin class II heavy chain (ISS)	16	11.6	70.3	5	+
Solyc01g088020	Protein transport protein sec31	41	14.8	121.5	11	+
Transport						
Solyc10g055630	Aquaporin	12	19	30.3	1	+
Solyc11g072880	Calcium-transporting ATPase	12	5	116.1	2	+
Solyc01g096060	Exportin, Cse1-like	11	4.3	109.6	4	+
Solyc07g017780	H^+-ATPase	37	14.9	106.4	5	+
Solyc06g071100	H^+-ATPase	79	25.8	105.0	3	+

ITAG accession[a]	Protein description	Score[b]	Coverage (%)	MW[c]	Unique peptides[d]	14-3-3 motif[e]
Solyc03g082940	Importin subunit beta	16	7.1	105.5	2	+
Solyc06g052030	Importin subunit beta	21	11.6	86.7	3	+
Solyc11g062190	Mitochondrial ADP_ATP carrier proteins	61	34.2	41.7	11	+
Solyc02g092440	Mitochondrial porin (Voltage-dependent anion channel) outer membrane protein	11	16.1	29.3	3	+
Solyc01g010760	Porin_voltage-dependent anion-selective channel protein	19	20.7	29.4	4	+
Solyc03g058920	Porin_voltage-dependent anion-selective channel protein	33	24	36.4	3	+
Solyc10g012050	Small conductance mechanosensitive ion channel family protein	47	2.6	54.4	1	+
Solyc03g097790	V-type proton ATPase subunit C	13	15.8	34.8	4	+
Solyc12g056110	V-type proton ATPase subunit E	28	20.6	26.1	1	-
Solyc08g008210	V-type proton ATPase subunit E	32	22	27.6	1	-
Respiration electron transport chain						
Solyc09g064450	NADH dehydrogenase (Ubiquinone)-binding domain	19	16.5	43.7	4	+
oxidation-reduction process						
Solyc05g005700	Aldehyde dehydrogenase 1	14	7.2	57.8	3	+
Antioxidant						
Solyc04g082460	Catalase	27	14.7	56.8	3	-
Solyc04g071900	Peroxidase	11	12.7	38.9	2	+
Unknown						
Solyc06g048440	Glycine rich protein	19	28.9	36.8	4	-
Solyc02g088260	Latex abundant protein	19	22.7	41.7	5	+
Solyc04g080140	Myxococcales GC_trans_RRR domain protein	16	10.8	72.9	4	+
Solyc03g025530	S-layer domain protein	13	6.9	102.8	3	+

[a] ITAG accession number of *Solanum lycopersicum* genes
[b] The score assigned by SEQUEST software after database searching
[c] Theoritical molecular weight of the identified protein
[d] Total number of detected unique peptides of the identified protein
[e] 14-3-3 binding sites predicted by the 14-3-3-Pred website: "+", corresponding protein has at least one 14-3-3 binding site, "-", corresponding protein has no 14-3-3 binding site.

Figure 9

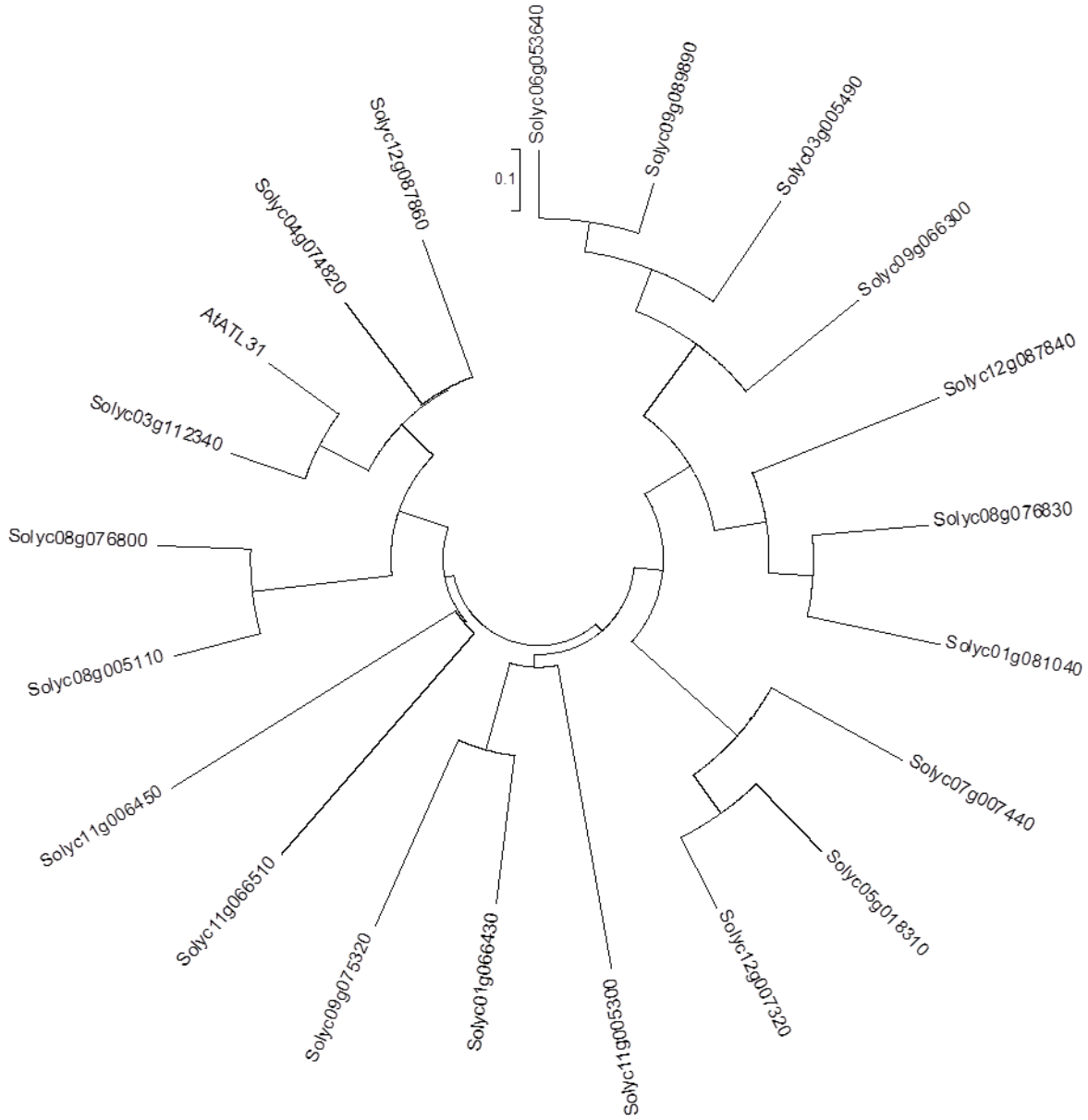
0.1
Solyc06g053640
Solyc09g089890
Solyc03g005490
Solyc09g066300
Solyc12g087840
Solyc08g076830
Solyc01g081040
Solyc07g007440
Solyc05g018310
Solyc12g007320
Solyc11g005300
Solyc01g066430
Solyc09g075320
Solyc11g066510
Solyc11g006450
Solyc08g005110
Solyc08g076800
Solyc03g112340
AtATL31
Solyc04g074820
Solyc12g087860

Figure 9. Phylogenetic analysis of tomato RING domain proteins homologous to Arabidopsis ATL31.

Phylogenetic tree was constructed using MEGA6 software with neighbor-joining method. Arrowhead indicates the gene assigned as *SlATL31*.

Figure 10

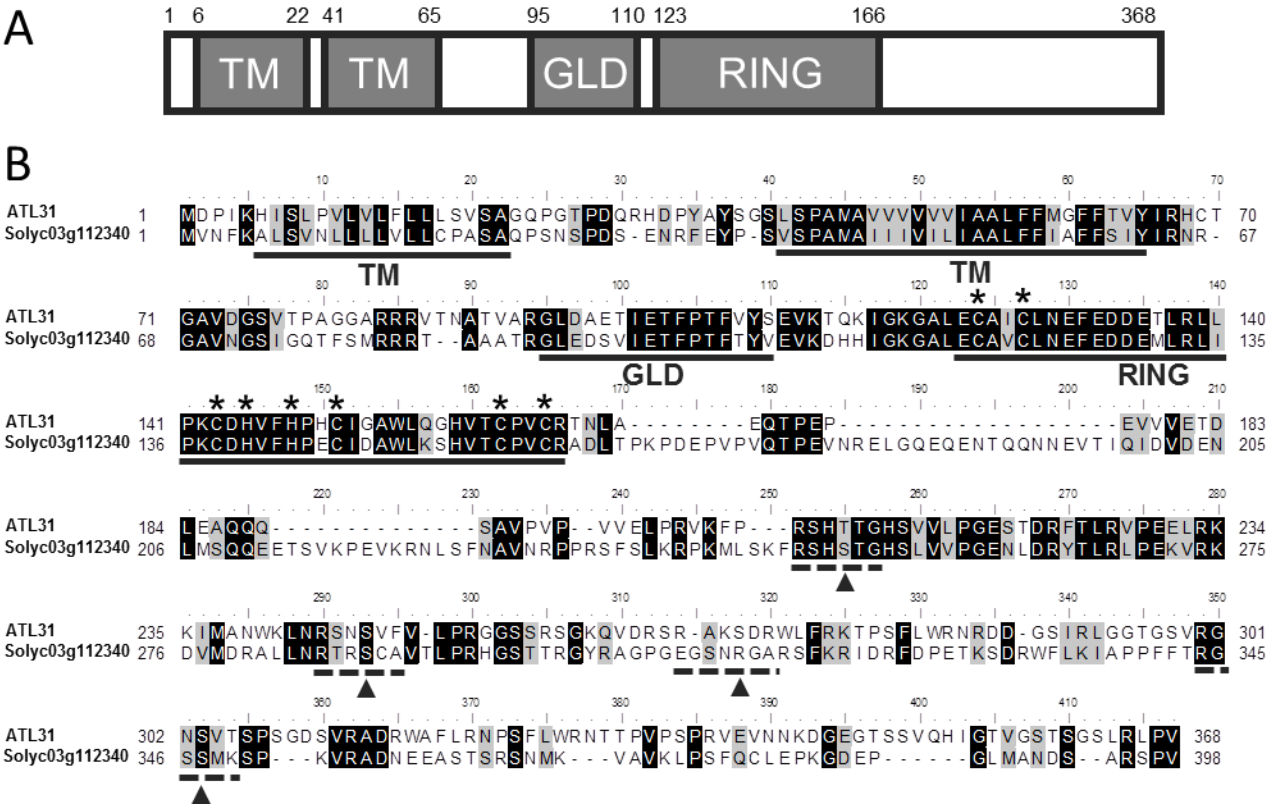
A
1 6 22 41 65 95 110 123 166 368
TM
TM
GLD
RING
B
ATL31 1 MDPIKHISLPVLVLFLLLSVSAGQPGTPDQRHDPYAYSGSLSPAMAVVVVVVIAALFFMGFFTVYIRHCT 70
Solyc03g112340 1 MVNFKALSVNLLLLVLLCPASAQPSNSPDS-ENRFEYP-SVSPAMAIIIVILIAALFFIAFFSIYIRNR- 67
TM
TM
ATL31 71 GAVDGSVTPAGGARRRVTNATVARGLDAETIETFPTFVYSEVKTQKIGKGALECAICLNEFEDDETLRLL 140
Solyc03g112340 68 GAVNGSIGQTFSMRRRT--AAATRGLEDSVIETFPTFTYVEVKDHHIGKGALECAVCLNEFEDDEMLRLI 135
GLD
RING
ATL31 141 PKCDHVFHPHCIGAWLQGHVTCPVCRTNLA--------EQTPEP--------------------EVVVETD 183
Solyc03g112340 136 PKCDHVFHPECIDAWLKSHVTCPVCRADLTPKPDEPVPVQTPEVNRELGQEQENTQQNNEVTIQIDVDEN 205
ATL31 184 LEAQQQ--------------SAVPVP--VVELPRVKFP---RSHTTGHSVVLPGESTDRFTLRVPEELRK 234
Solyc03g112340 206 LMSQQEETSVKPEVKRNLSFNAVNRPPRSFSLKRPKMLSKFRSHSTGHSLVVPGENLDRYTLRLPEKVRK 275
ATL31 235 KIMANWKLNRSNSVFV-LPRGGSSRSGKQVDRSR-AKSDRWLFRKTPSFLWRNRDD-GSIRLGGTGSVRG 301
Solyc03g112340 276 DVMDRALLNRTRSCAVTLPRHGSTTRGYRAGPGEGSNRGARSFKRIDRFDPETKSDRWFLKIAPPFFTRG 345
ATL31 302 NSVTSPSGDSVRADRWAFLRNPSFLWRNTTPVPSPRVEVNNKDGEGTSSVQHIGTVGSTSGSLRLPV 368
Solyc03g112340 346 SSMKSP---KVRADNEEASTSRSNMK---VAVKLPSFQCLEPKGDEP------GLMANDS--ARSPV 398

Figure 10. **Schematic diagram and alignment of Arabidopsis and tomato ATL31 proteins.**

(A) Schematic representation of the Arabidopsis ATL31 protein. TM, transmembrane-like hydrophobic region; GLD, highly conserved motif containing Gly-Leu-Asp residues; RING, a RING-H2 type zinc finger domain. (B) Amino acid sequence alignment of Arabidopsis and tomato ATL31 proteins. Asterisks indicate conserved Cys and His residues in the RING domain. Dashed underlines indicate the 14-3-3 binding sites on ATL31. Arrowheads indicate putative phosphorylated Ser or Thr residues in the 14-3-3 binding sites.

Figure 11

A

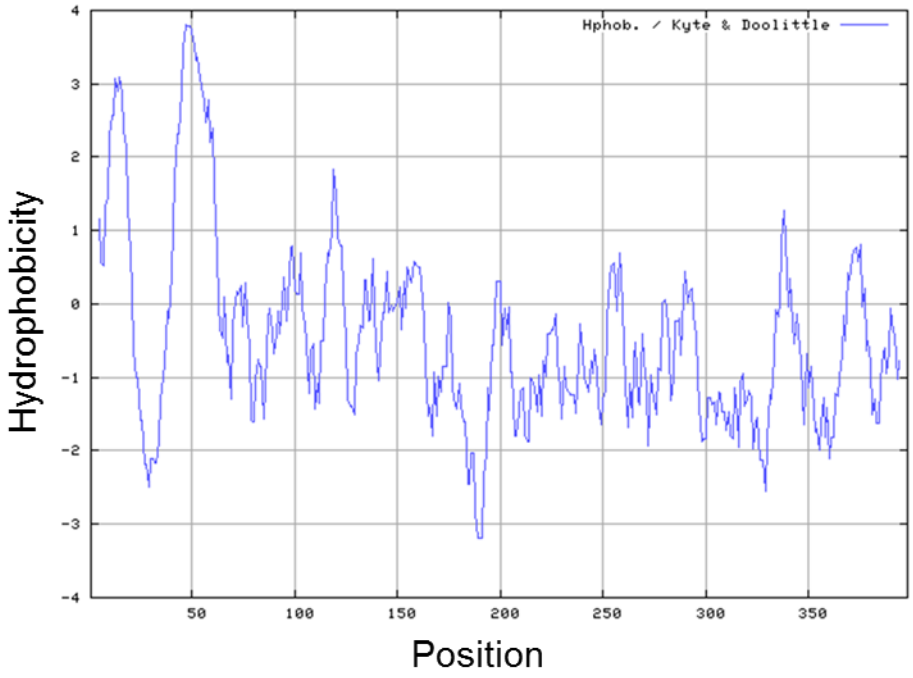
Hphob. / Kyte & Doolittle
Hydrophobicity
Position
4
3
2
1
0
-1
-2
-3
-4
50
100
150
200
250
300
350

B

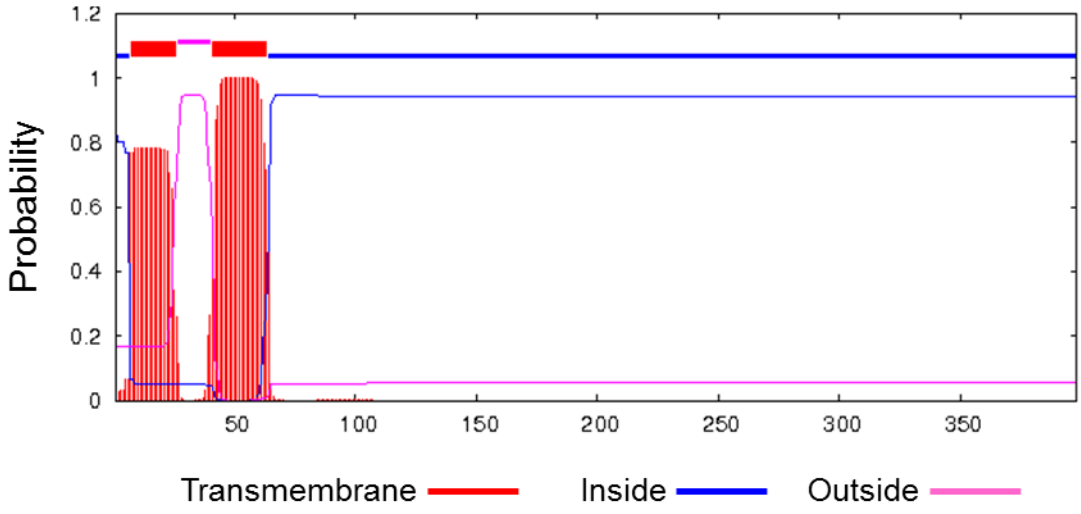
Probability
1.2
1
0.8
0.6
0.4
0.2
0
50
100
150
200
250
300
350
Transmembrane
Inside
Outside

Figure 11. Predicted transmembrane domain of Solyc03g112340 protein.

(A) Hydropathy profile of SlATL31 protein, as determined with ProtScale software (http://web.expasy.org/protscale/). (B) Predicted transmembrane region and topology of the Solyc03g112340, as determined with the TMHMM server v. 2.0 (http://www.cbs.dtu.dk/services/TMHMM/).

Figure 12

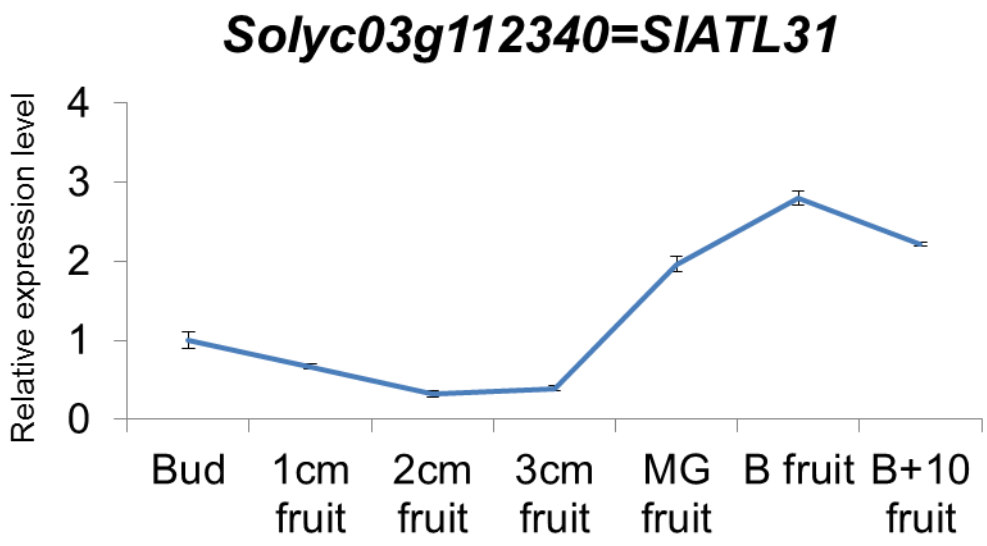
Solyc03g112340=SlATL31
Relative expression level
4
3
2
1
0
Bud
1cm fruit
2cm fruit
3cm fruit
MG fruit
B fruit
B+10 fruit

Figure 12. Expression pattern of *SlATL31* gene.

Relative expression level of *SlATL31* gene during fruit development were calculated based on the microarray data by The Tomato Genome Consortium. Relative expression levels were compared with that of Bud stage. MG, mature green. B, beaker. B+10, beaker +10 days.

Figure 13

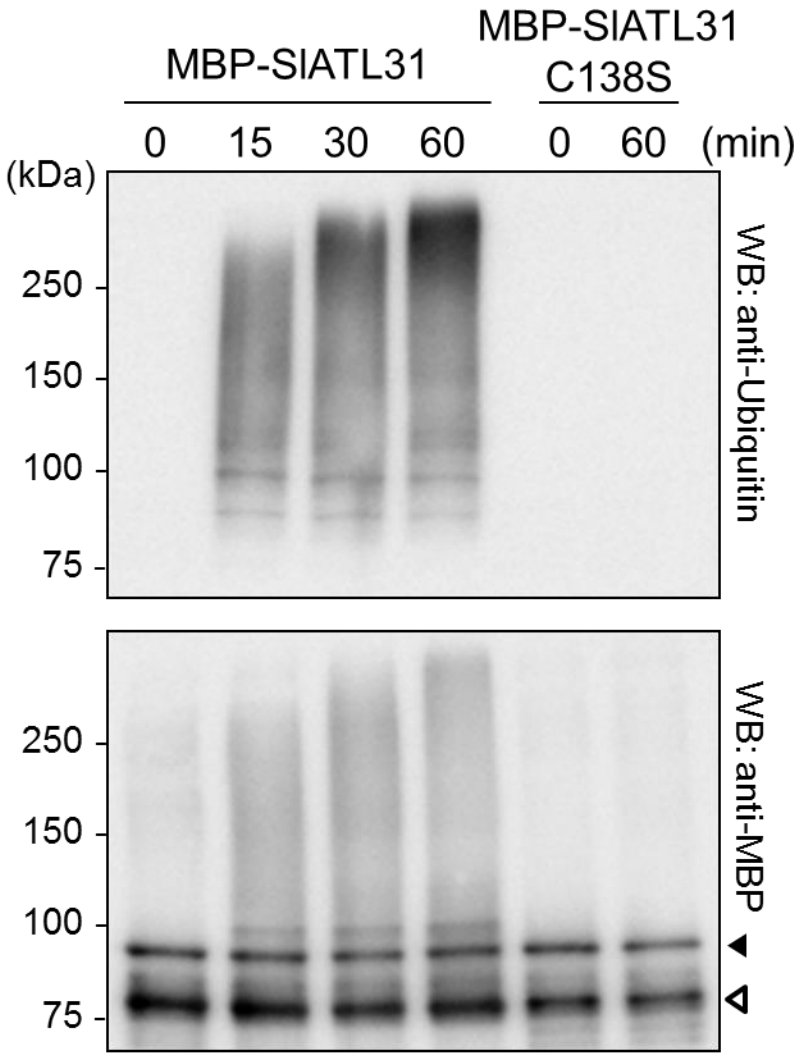
MBP-SlATL31
MBP-SlATL31 C138S
0 15 30 60 0 60 (min)
(kDa)
250
150
100
75
WB: anti-Ubiquitin
250
150
100
75
WB: anti-MBP

Figure 13. *In vitro* ubiquitination analysis of SlATL31 protein.

MBP-SlATL31 protein was incubated with E1, E2, ubiquitin and ATP for indicated time periods. Ubiquitination resulted in a heterogeneous collection of higher molecular mass proteins detected by western blotting with anti-ubiquitin (upper panel) and anti-MBP (lower panel) antibodies. The black arrowhead indicates the band representing the native forms of MBP-SlATL31 and the white arrowhead indicates the degraded SlATL31 fragment.

Figure 14

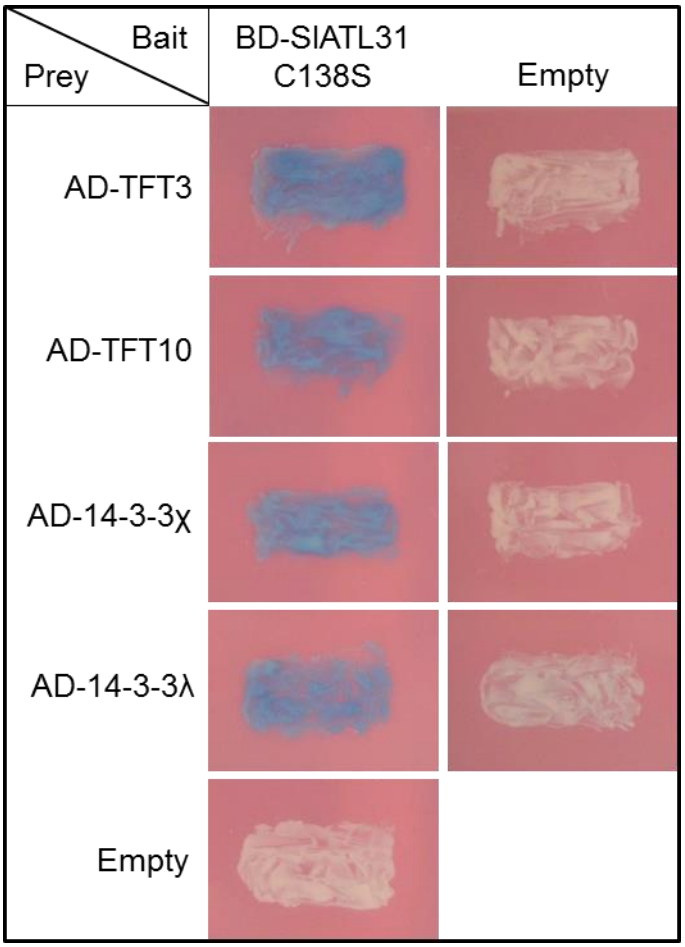
Bait
Prey
BD-SlATL31 C138S
Empty
AD-TFT3
AD-TFT10
AD-14-3-3χ
AD-14-3-3λ
Empty

Figure 14. Interaction analysis between SlATL31 and 14-3-3 proteins.

The *SlATL31C138S* construct fused with the LexA DNA binding domain (BD) and each full-length *14-3-3* isoform fused with the B42 transactivation domain (AD) were co-transformed into yeast cells. The interactions between SlATL31 and each 14-3-3 isoform were detected using *β*-galactosidase assay. Empty indicates negative controls consisting of the no fusion forms of bait and prey constructs.

Figure 15

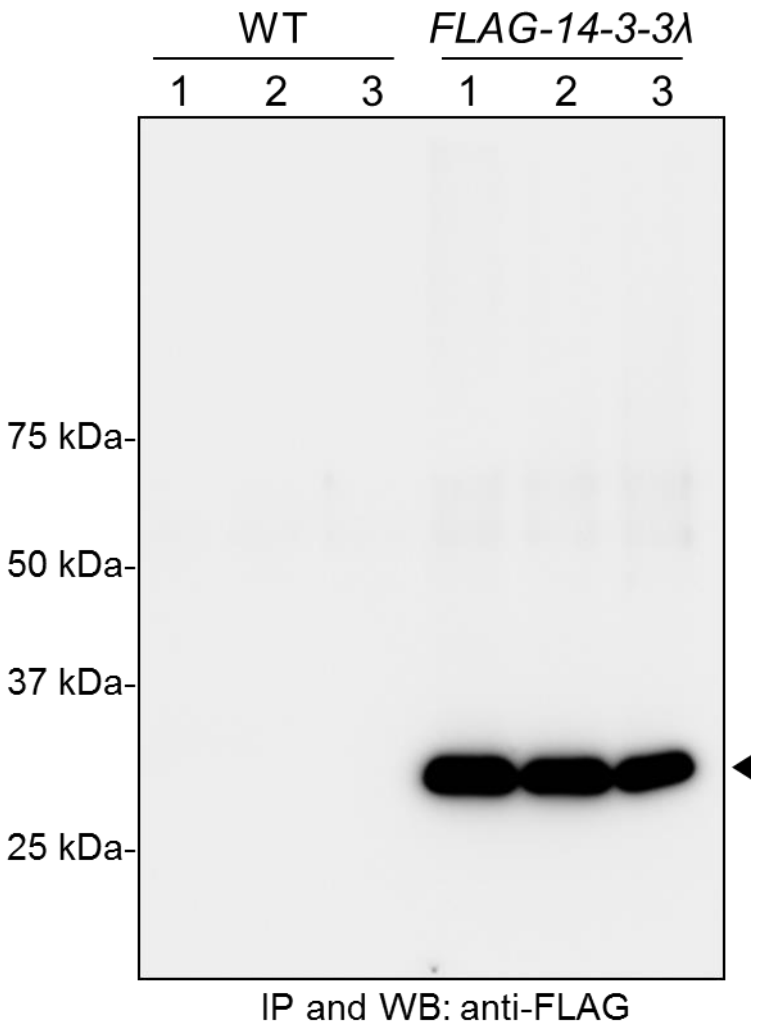
WT
FLAG-14-3-3λ
1
2
3
1
2
3
75 kDa-
50 kDa-
37 kDa-
25 kDa-
IP and WB: anti-FLAG

Figure 15. Purification of FLAG-14-3-3λ protein from transgenic tomato fruit.

Proteins were extracted from green expanding fruit and immunoprecipitated using anti-FLAG-beads. FLAG-14-3-3λ protein was detected by immunoblotting analysis using anti-FLAG antibody (arrowhead). The number of 1, 2 and 3 indicate three biological repeats.

Figure 16

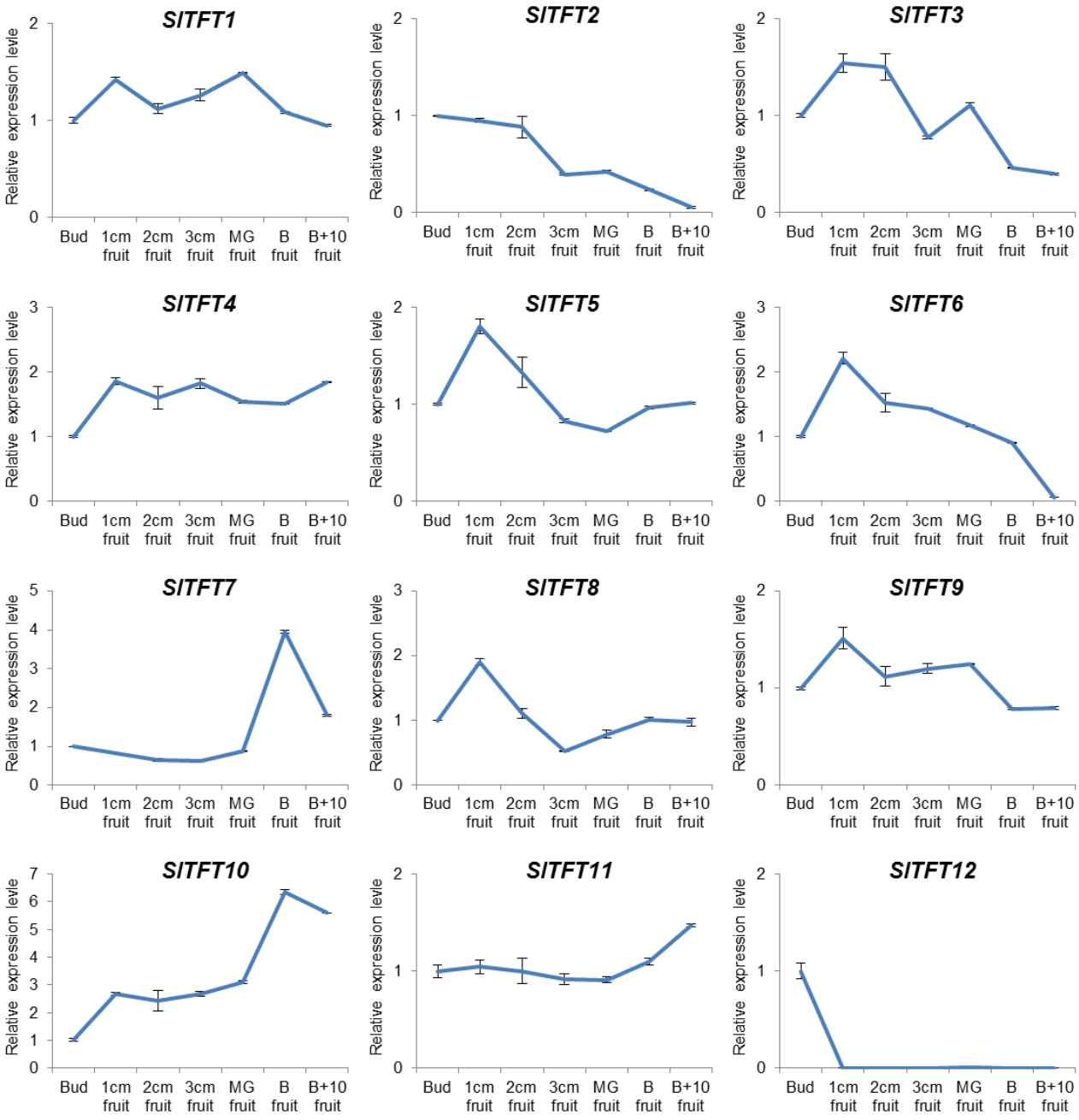
SlTFT1
SlTFT2
SlTFT3
SlTFT4
SlTFT5
SlTFT6
SlTFT7
SlTFT8
SlTFT9
SlTFT10
SlTFT11
SlTFT12
Relative expression levle
Bud
1cm fruit
2cm fruit
3cm fruit
MG fruit
B fruit
B+10 fruit

Figure 16. Expression patterns of *TFT* genes.

Relative expression levels of *TFT* genes during fruit development were calculated based on the microarray data by The Tomato Genome Consortium. Relative expression levels were compared with that of Bud stage. MG, mature green. B, beaker. B+10, beaker +10 days.

Figure 17

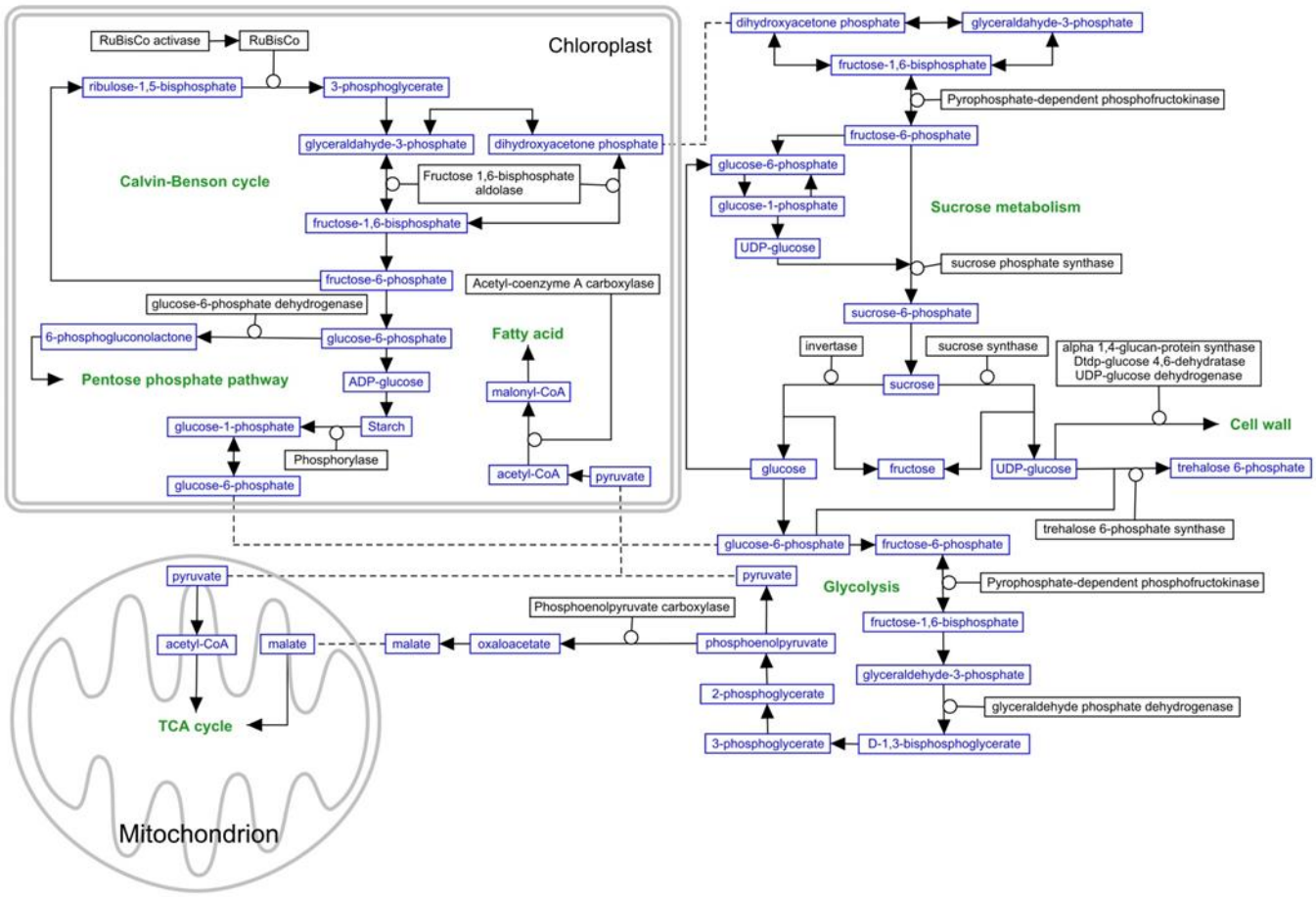
Chloroplast
RuBisCo activase
RuBisCo
ribulose-1,5-bisphosphate
3-phosphoglycerate
glyceraldahyde-3-phosphate
dihydroxyacetone phosphate
Calvin-Benson cycle
Fructose 1,6-bisphosphate aldolase
fructose-1,6-bisphosphate
fructose-6-phosphate
Acetyl-coenzyme A carboxylase
glucose-6-phosphate dehydrogenase
6-phosphogluconolactone
glucose-6-phosphate
Fatty acid
Pentose phosphate pathway
ADP-glucose
malonyl-CoA
glucose-1-phosphate
Starch
Phosphorylase
glucose-6-phosphate
acetyl-CoA
pyruvate
dihydroxyacetone phosphate
glyceraldahyde-3-phosphate
fructose-1,6-bisphosphate
Pyrophosphate-dependent phosphofructokinase
fructose-6-phosphate
glucose-6-phosphate
glucose-1-phosphate
Sucrose metabolism
UDP-glucose
sucrose phosphate synthase
sucrose-6-phosphate
invertase
sucrose synthase
alpha 1,4-glucan-protein synthase
Dtdp-glucose 4,6-dehydratase
UDP-glucose dehydrogenase
sucrose
Cell wall
glucose
fructose
UDP-glucose
trehalose 6-phosphate
trehalose 6-phosphate synthase
glucose-6-phosphate
fructose-6-phosphate
pyruvate
Glycolysis
Pyrophosphate-dependent phosphofructokinase
Phosphoenolpyruvate carboxylase
fructose-1,6-bisphosphate
pyruvate
acetyl-CoA
malate
malate
oxaloacetate
phosphoenolpyruvate
glyceraldehyde-3-phosphate
2-phosphoglycerate
glyceraldehyde phosphate dehydrogenase
TCA cycle
3-phosphoglycerate
D-1,3-bisphosphoglycerate
Mitochondrion

Figure 17. Summary of putative 14-3-3 target enzymes involved in carbon metabolism.

Blue boxes indicate metabolites and black boxes indicate putative 14-3-3 target enzymes identified in this study. Schematic model was constructed using PathVisio 3.2.1 (http://www. Pathvisio.org/).

Figure 18

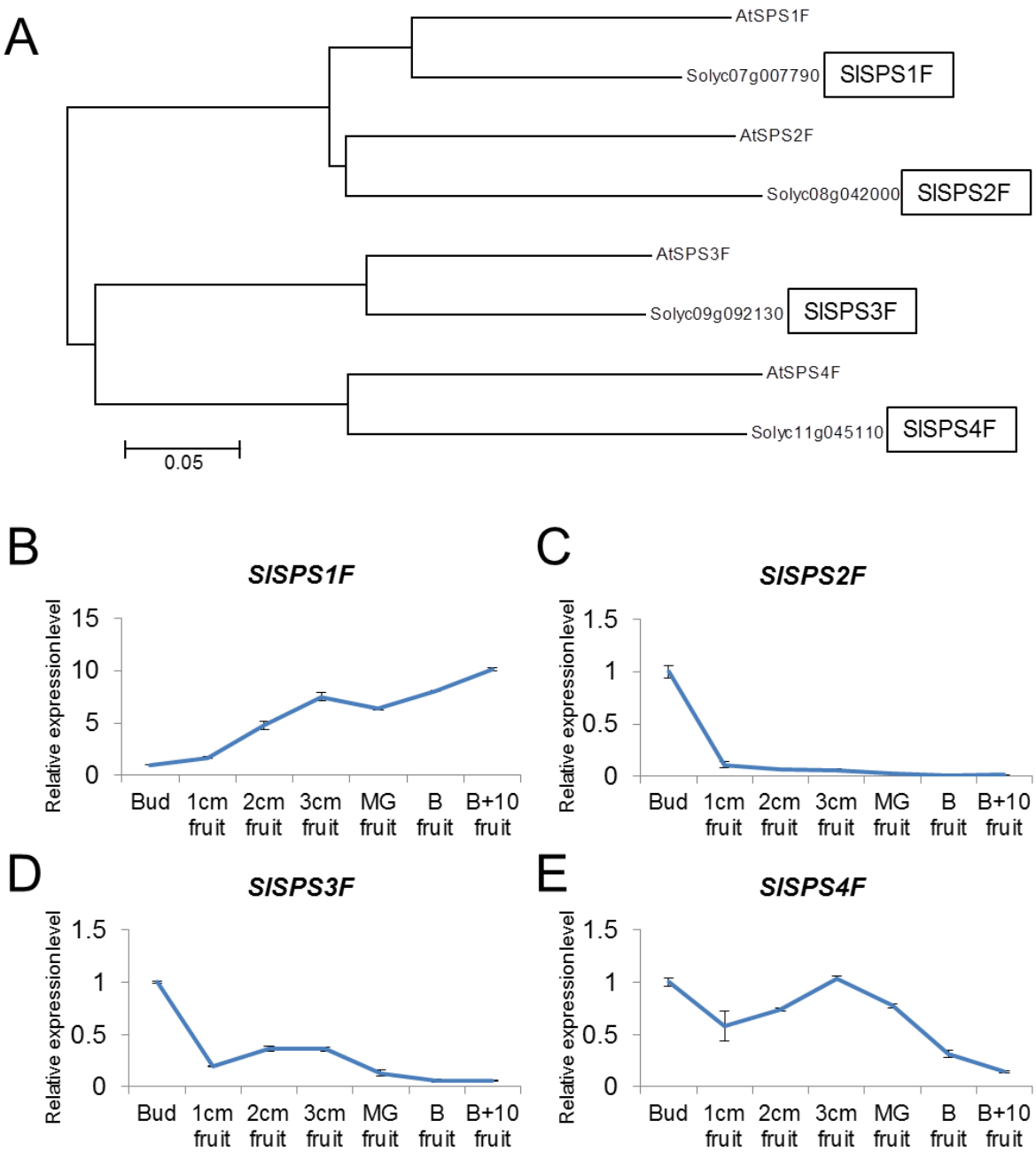
A
AtSPS1F
Solyc07g007790
SlSPS1F
AtSPS2F
Solyc08g042000
SlSPS2F
AtSPS3F
Solyc09g092130
SlSPS3F
AtSPS4F
Solyc11g045110
SlSPS4F
0.05
B
SlSPS1F
C
SlSPS2F
D
SlSPS3F
E
SlSPS4F
Relative expression level
Bud
1cm fruit
2cm fruit
3cm fruit
MG fruit
B fruit
B+10 fruit

Figure 18. Phylogenetic analysis and expression patterns of tomato *SPS* genes.

(A) Phylogenetic tree was constructed using neighbor-joining method with MEGA6 software. (B)-(E) Relative expression levels of tomato *SPS* genes during fruit development were calculated based on the microarray data by The Tomato Genome Consortium. Relative expression levels were compared with that of Bud stage. MG, mature green. B, beaker. B+10, beaker +10 days.

Figure 19

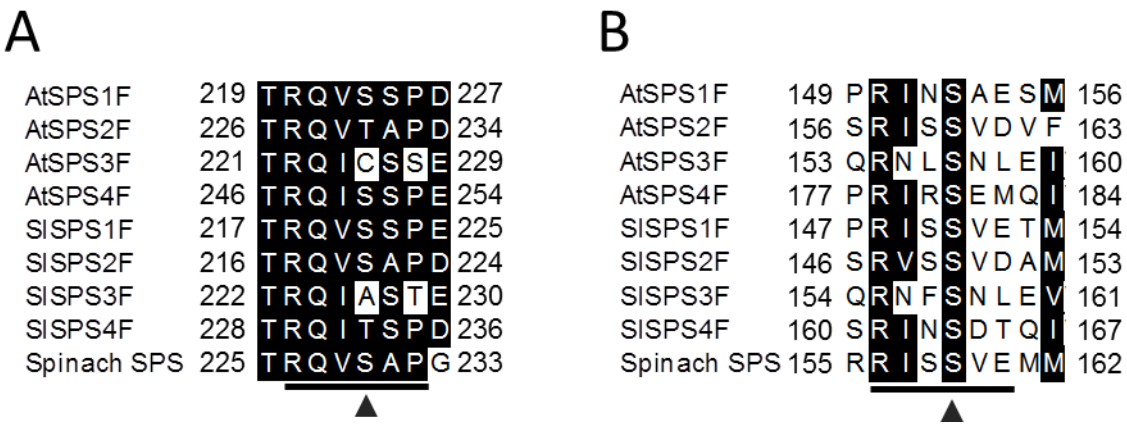
A
AtSPS1F 219 TRQVSSPD 227
AtSPS2F 226 TRQVTAPD 234
AtSPS3F 221 TRQICSSE 229
AtSPS4F 246 TRQISSPE 254
SlSPS1F 217 TRQVSSPE 225
SlSPS2F 216 TRQVSAPD 224
SlSPS3F 222 TRQIASTE 230
SlSPS4F 228 TRQITSPD 236
Spinach SPS 225 TRQVSAPG 233
B
AtSPS1F 149 PRINSAESM 156
AtSPS2F 156 SRISSVDVF 163
AtSPS3F 153 QRNLSNLEI 160
AtSPS4F 177 PRIRSEMQI 184
SlSPS1F 147 PRISSVETM 154
SlSPS2F 146 SRVSSVDAM 153
SlSPS3F 154 QRNFSNLEV 161
SlSPS4F 160 SRINSDTQI 167
Spinach SPS 155 RRISSVEMM 162

Figure 19. Amino acid sequence alignment of predicted 14-3-3 binding motifs in SPS proteins in Arabidopsis, tomato and spinach.

(A) 14-3-3 binding site containing Ser229 residue (arrowhead) of spinach SPS protein. (B) 14-3-3 binding site containing Ser157 residue (arrowhead) of tomato SlSPS3F protein. Underlined residues indicate the predicted 14-3-3 binding motif.

CONCLUDING REMAKERS

In Chapter I, I demonstrated that ABI1 regulates plant C/N response independent of ABA biosynthesis and canonical ABA signaling pathways. Firstly, I demonstrated that ABA biosynthesis is not activated in response to C/N stress condition, suggesting that the existence of a direct crosstalk between ABA signaling and C/N nutrient signal independent of ABA biosynthesis. Secondly, my results indicated that rather than canonical ABA signaling pathways, novel signaling pathways participated in the regulation of C/N response under ABI1 control. Moreover, this study also shades a light in the new regulatory function of ABI1, and further investigation of the ABI1-SnRK1 pathway is needed to understand the function of ABI1 in C/N stress condition.

In Chapter II, I isolated *SlATL31* gene in tomato and demonstrated that SlATL31 has ubiquitin ligase activity and interaction with tomato 14-3-3 proteins, suggesting the possibility that the SlATL31 functions as a ubiquitin ligase for 14-3-3 similarly to its Arabidopsis ortholog. Furthermore, proteomic analysis identified putative 14-3-3 target proteins involved in various metabolic and signaling pathways in tomato fruit. However, details of the molecular mechanism and physiological significance of the 14-3-3 interaction with each of these target proteins remain to be investigated. It will also be interesting to compare the composition of the 14-3-3 interactome network during the fruit developmental process. The involvement of ABI1 phosphatase activity to regulate the 14-3-3 interaction with the targets in tomato also should be investigated. That said my current study provides considerable insights into the sophisticated regulatory mechanism of fruit development via the post-translational regulation of key enzymes by 14-3-3 proteins and reveals them to be potential tools for engineering desirable fruit traits in tomato. They additionally provide important information linking ubiquitin ligases with downstream metabolic changes and as such provide a foundation for further studies in this understudied research area.

PUBLICATION LIST

1. **Yu Lu**, Yuki Sasaki, Xingwen Li, Izumi C. Mori, Takakazu Matsuura, Takashi Hirayama, Takeo Sato and Junji Yamaguchi (2015) ABI1 regulates carbon/nitrogen-nutrient signal transduction independent of ABA biosynthesis and canonical ABA signaling pathways in *Arabidopsis*. ***The Journal of Experimental Botany*** 66(9): 2763-2771.

2. **Yu Lu**, Junji Yamaguchi and Takeo Sato (2015) Integration of C/N-nutrient and multiple environmental signaling into the ABA signaling cascade. ***Plant Signaling & Behavior*** 10:12, e1048940.

3. **Yu Lu**, Shigetake Yasuda, Xingwen Li, Yoichiro Fukao, Takayuki Tohge, Alisdair R. Fernie, Chiaki Matsukura, Hiroshi Ezura, Takeo Sato, Junji Yamaguchi (2016) Characterization of ubiquitin ligase SlATL31 and proteomic analysis of 14-3-3 targets in tomato fruit tissue (*Solanum lycopersicum* L.). ***Journal of Proteomics*** 143 254-264.

PUBLICATION LIST (APPENDIX)

1. Shoki Aoyama, Thais Huarancca Reyes, Lorenzo Guglielminetti, **Yu Lu**, Yoshie Morita, Takeo Sato and Junji Yamaguchi (2014) C/N regulator ATL31 controls leaf senescence under elevated CO_2 and limited nitrogen condition. ***Plant Cell & Physiology*** 55(2): 293-305.

2. Shoki Aoyama, **Yu Lu**, Junji Yamaguchi, and Takeo Sato (2014) Regulation of senescence under elevated atmospheric CO_2 via ubiquitin modification. ***Plant Signaling & Behavior*** e28839.

3. Thais Huarancca Reyes, Andrea Scartazza, **Yu Lu**, Junji Yamaguchi, Lorenzo Guglielminetti (2016) Effect of carbon/nitrogen ratio on carbohydrate metabolism and light energy dissipation mechanisms in *Arabidopsis thaliana*. ***Plant Physiology and Biochemistry*** 105 195-202.